Supporting Information

Solid State Structures and Solution Behaviour of Tetranuclear Lanthanide(III) Carbonate-Bridged Coordination Compounds of Chiral 3+3 Amine Macrocycle

Karol Wydra,*[a] Vasyl Kinzhybalo,[b] Jerzy Lisowski*[a]

[a] *Department of Chemistry, University of Wrocław, 14 F. Joliot-Curie, 50-383 Wrocław, Poland*

[b] *Institute of Low Temperature and Structure Research, Okólna 2, 50-422 Wrocław, Poland*

Table of Contents

1. Experimental section 2
2. Single crystal X-ray diffraction 7
3. Powder X-ray diffraction 17
4. IR spectra 18
5. NMR spectrum of ligand $H_3\mathbf{L}^{\boldsymbol{R}}$ 19
6. NMR spectra of complex **2a** 20
7. ESI-MS spectra 23
8. NMR spectra of complex **1a** and the signals assignment 26
9. References 52

1. Experimental section

General Procedures

All reagents were purchased from commercial sources and were of reagent grade. Deuterated chloroform was dried prior to use by distillation from CaH_2 under nitrogen atmosphere. All other chemicals were used as received without further purification. The ligand $H_3\mathbf{L}^{R}$ was synthesized according to previously described procedure.[1-3]

NMR spectra were recorded on Jeol JNM-ECZ500R 500 MHz, Bruker Avance III 500 MHz, or Bruker Avance III 600 MHz spectrometers. All ESI-MS experiments were performed on Bruker Compact mass spectrometer equipped with standard ESI source. The measurements were performed using following instrument parameters: ESI capillary voltage: 3.5 kV, the nebulizing gas was nitrogen (flow rate: 3 L/min), desolvation temperature: 200 °C, sample flow rate: 3 µl/min, scan range (positive ion mode): 200-3000 *m/z*. Elemental analysis were obtained on CHNS Vario EL Cube (Elementar) instrument. Fourier transform infrared (FT-IR) spectra were taken on Bruker Vertex 70 FT-IR spectrometer using KBr method. Powder X-ray diffraction patterns were recorded from 5° to 40° by using PANalytical X'Pert Pro diffractometer in Bragg-Brentano geometry with CuKα radiation. The crystals of compounds **1a**-**3a** at room temperature undergo fast desolvation and easily decompose upon drying. Thus, PXRD experiments were carried out for well-grounded samples immersed in methanol/water (1:1, v/v) solvent mixture and loaded between two sealed Kapton foils.

Synthesis of the coordination compounds $[Ln_4(CO_3)_2(HL^{R})_2(NO_3)_2(H_2O)_4](NO_3)_2$ (1a-3a)

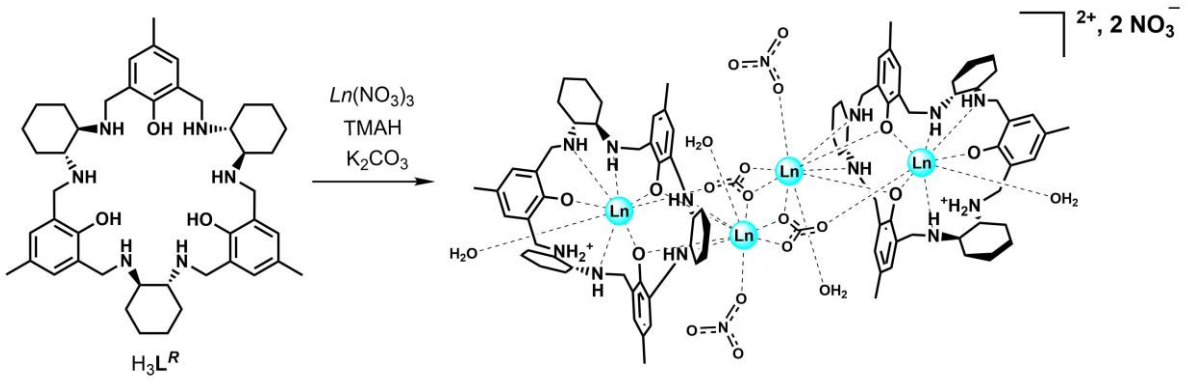

Sheme S1 Synthesis of the coordination compounds **1a**-**3a** (Ln^{3+} = Sm^{3+} for **1a**, Eu^{3+} for **2a** and Gd^{3+} for **3a**).

The series of coordination species **1a**-**3a** was obtained using different $Ln(NO_3)_3/H_3\mathbf{L}^{R}/K_2CO_3$/TMAH molar ratios of 2:1:1:2, 2:1:0.5:2 or 1.9:1:0.5:1.9, according to the same synthetic procedure (described below for the third reactants ratio; Scheme S1). Ligand

$H_3\mathbf{L}^{\boldsymbol{R}}$·2.8$CH_3OH$·0.6$H_2O$ (100.0 mg, 0.119 mmol) and lanthanide(III) nitrate hydrate (0.222 mmol; 98.9 mg of $Sm(NO_3)_3$·6H_2O (for **1a**), 95.2 mg of $Eu(NO_3)_3$·5H_2O (for **2a**), or 100.4 mg of $Gd(NO_3)_3$·6H_2O (for **3a**)) were dissolved in 10 mL of methanol and 3 mL of double distilled water, and then 25% methanol solution of tetramethylammonium hydroxide (TMAH; 94 µl, 0.222 mmol) and 0.87 M aqueous solution of K_2CO_3 (70 µl, 0.061 mmol) were added, respectively. The resulting light green-yellow (for **1a** and **3a**)/pale yellow (for **2a**) solution was stirred for 1 h at room temperature (RT) and then concentrated on rotatory evaporator until precipitate was formed. The mixture was stirred for 10 min and the obtained creamy (for **1a** and **3a**) or pale yellow (for **2a**) precipitate was filtered, washed three times with double distilled water/methanol mixture (1:1, v/v) and dried under vacuum for 24 h.

$[Sm_4(CO_3)_2(HL^R)_2(NO_3)_2(H_2O)_4](NO_3)_2$·2$H_2O$ (**1a**) Yield: 57.3 mg (38%). Elemental analysis: found: C 43.32, H 5.81, N 8.63. Calc. for $C_{92}H_{140}N_{16}O_{30}Sm_4$: C 43.31, H 5.53, N 8.78. **FT-IR:** (KBr pellet) ν_{max}/cm^{-1} 3430s;br, 3242m, 2933s, 2860s, 1630m, 1517m (ν(CO), CO_3^{2-}), 1476vs, 1383vs (ν(NO), NO_3^-), 1302vs;br, (1190-990)m, 927w, 866m, 792m. **^{1}H NMR**: (CD_3OD/D_2O 20:1 (v/v) solution, [**1a**]$_0$ = 16.5 mM, 500 MHz, 300 K): δ [ppm] = 9.87 (b, 2H, 30_b^a), 9.54 (b, 2H, 15_b^a), 8.71 (b, 2H, 14^a), 7.65 (b, 2H, 4^a), 7.49 (b, 2H, 6^a), 6.64 (b, 2H, 32^a), 5.65 (d, 2H, 45_a^a), 5.57 (b, 2H, 17^a), 5.00 (d, 2H, 45_b^a), 4.92 (b, 2H, 34^a), 4.83 (b, 2H, 29^a), 4.62 (b, 2H, 19^a), 4.47 (b, 4H, 9^a, 30_a^a), 4.20 (b, 2H, 15_a^a), 3.28 (b, 4H, 23_a^a, 44^a), 3.06 (b, 4H, 13_b^a, 28_a^a), 2.62 (s, 6H, 8^a), 2.54 (b, 2H, 12_a^a), 2.35 (b, 8H, 10_a^a, 11_b^a, 13_a^a, 43_a^a), 2.27 (b, 4H, 11_a^a, 28_b^a), 2.25 (b, 2H, 1_a^a), 2.11 (b, 2H, 25_b^a), 2.08 (b, 2H, 10_b^a), 1.95 (b, 4H, 12_b^a, 27_a^a), 1.68 (b, 2H, 27_b^a), 1.62 (b, 2H, 26_a^a), 1.58 (b, 2H, 42_b^a), 1.40 (s, 2H, 37^a), 1.35 (b, 2H, 23_b^a), 1.33 (b, 4H, 1_b^a, 43_b^a), 1.21 (b, 2H, 41_b^a), 1.03 (s, 6H, 22^a), 0.97 (b, 2H, 25_a^a), 0.83 (b, 2H, 39^a), 0.75 (b, 2H, 42_a^a), 0.67 (b, 2H, 41_a^a), 0.61 (b, 2H, 26_b^a), 0.59 (b, 2H, 40_b^a), 0.27 (b, 2H, 38_b^a), -0.12 (b, 2H, 38_a^a), -0.42 (b, 2H, 24^a), -0.61 (b, 2H, 40_a^a). **^{13}C NMR**: (CD_3OD/D_2O 20:1 (v/v) solution, [**1a**]$_0$ = 16.5 mM, 126 MHz, 300 K): δ [ppm] = 190.48 (C_{46}^a), 171.16 (C_2^a), 162.74 (C_{36}^a), 153.89 (C_{21}^a), 133.25 (C_6^a), 131.83 (C_4^a), 131.62 (C_{32}^a), 131.07 (C_x^a, C_{17}^a, C_{34}^a), 128.49 (C_{19}^a), 128.11 (C_x^a), 126.32 (C_5^a), 126.23 (C_{33}^a, C_x^a), 125.36 (C_x^a), 124.65 (C_{18}^a), 119.12 (C_x^a), 116.92 (C_3^a), 66.39 (C_{14}^a), 65.92 (C_{29}^a), 64.77 (C_9^a), 61.48 (C_{24}^a), 60.84 (C_{39}^a), 57.72 (C_{44}^a), 50.91 (C_{45}^a), 50.65 (C_{23}^a), 49.64 (C_1^a, C_{38}^a), 49.07 (C_{15}^a), 47.24 (C_{30}^a), 33.04 (C_{10}^a), 32.58 (C_{25}^a), 31.70 (C_{40}^a), 31.14 (C_{13}^a, C_{28}^a), 27.55 (C_{11}^a), 27.03 (C_{27}^a), 26.89 (C_{12}^a), 26.44 (C_{43}^a), 26.03 (C_{26}^a), 25.38 (C_{41}^a), 24.02 (C_{42}^a), 20.95 (C_8^a), 19.93 (C_{37}^a), 19.29 (C_{22}^a). **ESI-MS:** (*m/z*) 2394.68 $[Sm_4\mathbf{L}^{\boldsymbol{R}}_2(CO_3)_2(NO_3)_2(H_2O)_3+Na]^+$, 1166.36 $[Sm_4\mathbf{L}^{\boldsymbol{R}}_2(CO_3)_2(NO_3)(H_2O)_3+Na]^{2+}$, 951.44 $[Sm(H_2\mathbf{L}^{\boldsymbol{R}})(NO_3)]^+$, 756.91 $[Sm_4\mathbf{L}^{\boldsymbol{R}}_2(CO_3)_2(H_2O)_3+Na]^{3+}$, 742.24 $[Sm_4\mathbf{L}^{\boldsymbol{R}}(H\mathbf{L}^{\boldsymbol{R}})(CO_3)_2(CH_3OH)]^{3+}$, 549.18 $[Sm_2\mathbf{L}^{\boldsymbol{R}}(NO_3)]^{2+}$, 444.73 $[Sm(H_2\mathbf{L}^{\boldsymbol{R}})]^{2+}$.

$[Eu_4(CO_3)_2(HL^R)_2(NO_3)_2(H_2O)_4](NO_3)_2$·3$CH_3OH$·$H_2O$ (**2a**) Yield: 44.0 mg (28%). Elemental analysis: found: C 43.44, H 6.09, N 8.76. Calc. for $C_{95}H_{150}Eu_4N_{16}O_{32}$: C 43.28, H 5.74, N 8.50. **FT-IR:** (KBr pellet) ν_{max}/cm^{-1} 3430s;br, 3248m, 2933s, 2860s, 1630m, 1523m (ν(CO), CO_3^{2-}), 1476vs, 1383vs (ν(NO), NO_3^-), 1302vs;br, (1190-990)w, 927w, 866m, 792m.**^{1}H NMR**: (CD_3OD/D_2O 20:1 v/v solution, [**2a**]$_0$ = 5.3 mM, 500 MHz, 300 K): δ [ppm] = 38.12 (b, 2H, N*H*), 22.44 (b, 2H), 17.82 (b, 2H), 14.28 (b, 4H), 13.91 (b, 4H), 11.80 (b, 2H), 10.31 (b, 2H), 9.16 (b, 2H), 8.52 (b, 2H), 7.79 (b, 2H), 7.20 (s, 6H, CH_3), 6.64 (b, 2H), 6.41 (b, 4H), 6.09 (b, 2H), 4.34 (s,

6H, CH_3), 4.03 (b, 2H), 3.06 (b, 2H), 1.94 (b, 4H), 1.09 (b, 2H), 0.33 (b, 2H), -0.12 (b, 2H), -0.40 (b, 2H), -0.68 (b, 2H), -1.27 (b, 2H), -1.32 (b, 2H), -1.46 (b, 6H), -1.68 (b, 2H), -1.79 (b, 2H), -1.94 (b, 2H), -1.99 (b, 2H), -2.06 (b, 2H), -3.21 (b, 2H), -3.40 (s, 6H, CH_3; b, 2H), -3.55 (b, 2H), -3.65 (b, 2H), -4.09 (b, 2H), -4.41 (b, 2H), -5.16 (b, 2H), -10.11 (b, 2H), -12.32 (b, 2H), -17.31 (b, 2H), -17.52 (b, 2H), -23.21 (b, 2H), -24.29 (b, 2H), -28.10 (b, 2H). ESI-MS (*m/z*) 2399.70 $[Eu_4\mathbf{L}^{\boldsymbol{R}}_2(CO_3)_2(NO_3)_2(H_2O)_3+Na]^+$, 1168.87 $[Eu_4\mathbf{L}^{\boldsymbol{R}}_2(CO_3)_2(NO_3)(H_2O)_3+Na]^{2+}$, 952.45 $[Eu(H_2\mathbf{L}^{\boldsymbol{R}})(NO_3)]^+$, 758.58 $[Eu_4\mathbf{L}^{\boldsymbol{R}}_2(CO_3)_2(H_2O)_3+Na]^{2+}$, 744.58 $[Eu_4\mathbf{L}^{\boldsymbol{R}}(H\mathbf{L}^{\boldsymbol{R}})(CO_3)_2(CH_3OH)]^{3+}$, 550.68 $[Eu_2\mathbf{L}^{\boldsymbol{R}}(NO_3)]^{2+}$, 445.23 $[Eu(H_2\mathbf{L}^{\boldsymbol{R}})]^{2+}$.

$[Gd_4(CO_3)_2(HL^R)_2(NO_3)_2(H_2O)_4](NO_3)_2\cdot4CH_3OH\cdot3H_2O$ (**3a**) Yield: 50.0 mg (31%). Elemental analysis: found: C 42.31, H 6.13, N 8.43. Calc. for $C_{96}H_{158}Gd_4N_{16}O_{35}$: C 42.31,H 5.84, N 8.22. **FT-IR:** (KBr pellet) ν_{max}/cm^{-1} 3423s;br, 3248m, 2934s, 2860s, 1631m, 1523m (ν(CO), CO_3^{2-}), 1476vs, 1383vs (ν(NO), NO_3^-), 1302vs;br, (1190-990)m, 927w, 866m, 792m. ESI-MS (*m/z*) 2421.71 $[Gd_4\mathbf{L}^{\boldsymbol{R}}_2(CO_3)_2(NO_3)_2(H_2O)_3+Na]^+$, 1179.87 $[Gd_4\mathbf{L}^{\boldsymbol{R}}_2(CO_3)_2(NO_3)(H_2O)_3+Na]^{2+}$, 765.92 $[Gd_4\mathbf{L}^{\boldsymbol{R}}_2(CO_3)_2(H_2O)_3+Na]^{3+}$, 751.26 $[Gd_4\mathbf{L}^{\boldsymbol{R}}(H\mathbf{L}^{\boldsymbol{R}})(CO_3)_2(CH_3OH)]^{3+}$, 556.69 $[Gd_2\mathbf{L}^{\boldsymbol{R}}(NO_3)]^{2+}$, 447.73 $[Gd(H_2\mathbf{L}^{\boldsymbol{R}})]^{2+}$.

Crystal Structures Determination

The crystals of **1a**-**3a** were grown upon slow evaporation of filtrates from the syntheses, while those of $\mathbf{2a}_{0.5}\mathbf{2a'}_{0.5}$ and $\mathbf{3a}_{0.5}\mathbf{3a'}_{0.5}$ were obtained from the slowly evaporated methanol-water solutions of $Ln(NO_3)_3/H_3\mathbf{L}^{\boldsymbol{R}}$/TEA/TMAB (TEA = triethylamine; TMAB = tetramethylammonium bicarbonate) in a 1.8:1:3:0.8 molar ratio. The single-crystal X-ray diffraction data were collected at 100(2) K on Rigaku XtaLAB Synergy R, DW system, (HyPix-Arc 150 detector) and Agilent Technologies, Gemini ultra (Ruby CCD detector) *κ*-geometry four-circle diffractometers with graphite or mirror monochromated MoK_α or CuK_α radiation (see details in Table S1). Data collection, cell refinement, data reduction and analysis were carried out with CrysAlisPRO.[4] Analytical or gaussian absorption correction was applied to the data with CrysAlisPRO. The structure of **2a** was solved by direct methods using SHELXS[5] and refined on F^2 by full-matrix least-squares technique using SHELXL.[6] The crystals of **1a** and **3a**, as well as $\mathbf{2a}_{0.5}\mathbf{2a'}_{0.5}$ and $\mathbf{3a}_{0.5}\mathbf{3a'}_{0.5}$ are isomorphic with **2a**, hance their structures were refined, starting from the coordinates of fully-occupied non-H atoms taken from **2a**. All fully occupied and some of the partially occupied/disordered non-H atoms were refined anisotropically (see details in the CIF files). The C- and N-bound H-atoms were placed in geometrically calculated positions and refined using a riding model, with C−H = 0.95-1.00 Å and N−H = 0.91-1.00 Å, and with U_{iso}(H) = 1.2 U_{eq}(C,N) for NH, NH_2, CH, and CH_2, and U_{iso}(H) = 1.5U_{eq}(C) for CH_3. The methanol hydroxyl H-atoms were included using geometrical considerations and constrained with AFIX 3, AFIX 83 or AFIX 147 instructions. The water H-atoms were located in difference Fourier maps and refined with O−H and H···H distances restrained to 0.840(1) Å and 1.330(2) or 1.330(1) Å, respectively, and with U_{iso}(H) = 1.5U_{eq}(O), and then the riding model constraint

were applied (AFIX 3 instruction in SHELXL). Positions of H-atoms for some of the partially occupied water molecules were not found in difference Fourier maps.

The coordination cations $[Ln_4(H\mathbf{L}^{R})_2(CO_3)_2(NO_3)_2(H_2O)_4]^{2+}$ in **1a**-**3a** lie in a special position, that is on a 2-fold axis passing between two carbonate bridges. The asymmetric units comprise thus half of the coordination cations, one non-coordinating nitrate ion and half of the solvent molecules in comparison to the crystals formula. The two positions of axial ligands coordinated to *Ln*2 in the crystals of **1a**-**3a** were found to be substitutionally disordered with nitrate anion and water molecule sharing the same position (with site occupancy factor, SOF = 0.5). Additionally, in one of the axial site in **1a** the nitrate ion is disordered in two position, with SOF = 0.25. The final models consider that at one side of the complex the *Ln*2 is coordinated by H_2O and the *Ln*2^{i} (with atom coordinates (i) -x+1, y, -z+1) by NO_3^- (see Fig. S7). At the opposite side of the complex the *Ln*2 is coordinated by NO_3^- and the *Ln*2^{i} by H_2O. As a consequence, the $[Ln_4(H\mathbf{L}^{R})_2(CO_3)_2(NO_3)_2(H_2O)_4]^{2+}$ cation is of C_1 symmetry and exhibits two different orientations in the crystal lattice that are almost but not quite related by the 2-fold axis (for those two orientations the differences results only from a reversed set of axial ligands).

In the crystals of **2a**$_{0.5}$**2a'**$_{0.5}$ and **3a**$_{0.5}$**3a'**$_{0.5}$ the uncoordinated nitrate ion was found to be partially occupied, sharing the site with two partially occupied water molecules with O4W or O5W atoms (for the latter water molecule SOF = 0.1 and 0.15, respectively). The substitutionally disordered position was initially refined with SOFs = 0.524(14) (NO_3^-) or 0.476(14) (H_2O with O4*W*) for **2a**$_{0.5}$**2a'**$_{0.5}$, and 0.506(13) (NO_3^-) or 0.494(13) (H_2O with O4*W*) for **3a**$_{0.5}$**3a'**$_{0.5}$, and then was constrained with SOFs = 0.5 (NO_3^-/H_2O) for **2a**$_{0.5}$**2a'**$_{0.5}$ and SOFs = 0.5(NO_3^-)/0.4(H_2O) for **3a**$_{0.5}$**3a'**$_{0.5}$. This may indicate the presence of an equimolar amount of the coordination cation $[Ln_4(H\mathbf{L}^{R})_2(CO_3)_2(NO_3)_2(H_2O)_4]^{2+}$ and the neutral complex $[Ln_4\mathbf{L}^{R}_2(CO_3)_2(NO_3)_2(H_2O)_4]$, both lying on the special position of a 2-fold axis (SOF = 0.5) (however, the presence of partially occupied hydroxide anion, resulting in the overall compounds formulae of $[Ln_4(H\mathbf{L}^{R})_2(CO_3)_2(NO_3)_2(OH)(H_2O)_3](NO_3)$ or $[Ln_4(H\mathbf{L}^{R})_2(CO_3)_2(NO_3)_2(H_2O)_4](NO_3)(OH)$, cannot be excluded). The coordination species are in a discrete positional disorder, indicated by the substitutional disorder of four axial H_2O/NO_3^- positions and the occupancy of one of the NH_2^+ hydrogen atoms, that was constrained to be 0.5. The asymmetric units of the crystals comprise thus half of the averaged cations $[Ln_4(H_{0.5}\mathbf{L}^{R})_2(CO_3)_2(NO_3)_2(H_2O)_4]^+$, half of the nitrate anion and disordered solvent molecules (see CIF files for details). The finally accepted formula of the crystals are given in Table S1.

One of the phenolic rings in the bis-deprotonated macrocycles $(H\mathbf{L}^{R})^{2-}$ in **1a** and **3a** was found to be slightly disordered into two positions and was refined anisotropically, with SOF 0.528(17) and 0.472(17) in **1a**, and SOF 0.63(2) and 0.37(2) in **3a**. All the CH_3OH in **1a**-**3a** are disordered or partially occupied, except the molecule with O1*M* atom, present in each of the crystals. The second CH_3OH in **1a**-**3a** is located close to the special position and was refined in three sites in **1a**, with SOF = 0.2 (O2*MA*-C2*MA*), 0.25 (O2*MB*-C2*MB*) and 0.15 (O2*MC*-C2*MC*), while in **2a** and **3a** was refined in two positions, with SOF = 0.5 (O2*MA*-C2*MA*) and 0.25 (O2*MB*-

C2*MB*) for both crystals. Another site in **2a** and **3a** is partially occupied (SOF = 0.5) by CH_3OH (O3*M*-C3*M*), and in **1a** the same site is shared by H_2O with O9W (SOF = 0.2) and CH_3OH disordered in two positions (O3*MA*-C3*MA*/O3*MB*-C3*MB*), with SOFs fixed at 0.15. The remaining methanol molecule in **1a**, which also shares the site with H_2O (O10*W*; SOF = 0.15), is severely distorted and was refined in four positions, with SOFs constrained to 0.25, 0.2, 0.2 and 0.15 for O4*MA*-C4*MA*, O4*MB*-C4*MB*, O4*MC*-C4*MC* and O4*MD*-C4*MD*, respectively. Each of the remaining CH_3OH in **2a** and **3a** are disordered. In **2a** one out of three molecules were refined in three positions (SOF = 0.25/0.2/0.2 for O5*MA*-C5*MA*/O5*MB*-C5*MB*/O5*MC*-C5*MC*), while the last two share their sites with water molecules (see CIF flies) and are disordered in two positions, with SOF = 0.5/0.25 for O4*MA*-C4*MA*/O4*MB*-C*4MB* and SOFs = 0.15 for O6*MA*-C6*MA*/O6*MB*-C6*MB*. In the case of **3a** there are four remaining methanol molecules, three of them were refined in two positions (SOF = 0.5/0.25 for O4*MA*-C4*MA*/O4*MB*-C4*MB*, SOF = 0.3/0.25 for O5*MA*-C5*MA*/ O5*MB*-C5*MB*, and SOF = 0.35/0.3 for O7*MA*-C7*MA*/O7*MB*-C7*MB*), while the last one was found to be disordered over four positions with SOF = 0.2, 0.15, 0.15, and 0.15 for O6*MA*-C6*MA*, O6*MB*-C6*MB*, O6*MC*-C6*MC*, and O6*MD*-C6*MD*, respectively. Some of the sites were also shared by partially occupied water molecules. All water molecules in **1a**-**3a**, except the H_2O (with O1*W*) coordinated to *Ln*1, are partially occupied or disordered (for further details see CIF files). The finally accepted formula for the crystals of **1a**-**3a** are given in Table S1, although the amount of solvent molecules should be treated as rough approximation.

CCDCs no. 2267814 (for **1a**), 2267816 (for **2a**), 2267812 (for **3a**), 2267813 (for **2a**$_{0.5}$**2a'**$_{0.5}$) and 2267815 (for **3a**$_{0.5}$**3a'**$_{0.5}$) contains the supplementary crystallographic data in this article. These data can be obtained free of charge from The Cambridge Crystallographic Data Centre (www.ccdc.cam.ac.uk/structures.).

Table S1 Crystallographic data for the crystals.

	$[Sm_4(HL^R)_2(CO_3)_2(NO_3)_2(H_2O)_4](NO_3)_2{\cdot}5.4CH_3OH{\cdot}6H_2O$ (**1a**)	$[Eu_4(HL^R)_2(CO_3)_2(NO_3)_2(H_2O)_4](NO_3)_2{\cdot}7.9CH_3OH{\cdot}6H_2O$ (**2a**)	$[Gd_4(HL^R)_2(CO_3)_2(NO_3)_2(H_2O)_4](NO_3)_2{\cdot}9.7CH_3OH{\cdot}3.2H_2O$ (**3a**)	$[Eu_4(HL^R)_2(CO_3)_2(NO_3)_2(H_2O)_4]_{0.5}[Eu_4(L^R)_2(CO_3)_2(NO_3)_2(H_2O)_4]_{0.5}(NO_3){\cdot}6.1CH_3OH{\cdot}7.7H_2O$ (**2a$_{0.5}$2a'$_{0.5}$**)	$[Gd_4(HL^R)_2(CO_3)_2(NO_3)_2(H_2O)_4]_{0.5}[Gd_4(L^R)_2(CO_3)_2(NO_3)_2(H_2O)_4]_{0.5}(NO_3){\cdot}6.38CH_3OH{\cdot}6.7H_2O$ (**3a$_{0.5}$3a'$_{0.5}$**)
CCDC No.	2267814	2267816	2267812	2267813	2267815
Chemical formula	$C_{97.4}H_{169.6}N_{16}O_{39.4}Sm_4$	$C_{99.9}H_{179.6}Eu_4N_{16}O_{41.9}$	$C_{101.7}H_{181.2}Gd_4N_{16}O_{40.9}$	$C_{98.1}H_{174.8}Eu_4N_{15}O_{38.8}$	$C_{98.38}H_{173.92}Gd_4N_{15}O_{38.08}$
Molecular weight	2796.68	2883.23	2911.62	2793.16	2805.27
Crystal system, space group	Monoclinic, *C*2	Monoclinic, *C*2	Monoclinic, *C*2	Monoclinic, *C*2	Monoclinic, *C*2
Temperature (K)	100(2)	100(2)	100(2)	100(2)	100(2)
a, *b*, *c* (Å)	19.801(4), 16.681(3), 19.381(4)	20.006(3), 16.864(2), 19.373(3)	19.967(4), 16.817(3), 19.356(4)	20.085(3), 16.869(2), 19.367(2)	20.134(5), 16.859(4), 19.337(5)
α, β, γ (°)	90, 104.09(2), 90	90, 104.19(2), 90	90, 104.33(2), 90	90, 103.93(2), 90	90, 103.91(3), 90
V (Å^3)	6209(2)	6337(2)	6297(2)	6369(2)	6371(3)
Z	2	2	2	2	2
Radiation type	Cu *K*α	Mo *K*α	Mo *K*α	Cu *K*α	Cu *K*α
μ (mm^{-1})	14.68	2.04	2.16	14.55	13.91
Diffractometer	Rigaku XtaLAB Synergy R, DW system	Rigaku XtaLAB Synergy R, DW system	Agilent Technologies Xcalibur, Gemini ultra	Rigaku XtaLAB Synergy R, DW system	Rigaku XtaLAB Synergy R, DW system
Absorption correction	analytical	analytical	analytical	gaussian	gaussian
T_{min}, T_{max}	0.090, 0.409	0.736, 0.872	0.591, 0.743	0.306, 0.644	0.067, 0.445
No. of measured, independent and observed [$I > 2\sigma(I)$] reflections	57173, 12550, 12060	125965, 28492, 27166	25214, 14375, 13286	55479, 12922, 12310	107537, 12557, 12130
R_{int}	0.029	0.019	0.020	0.028	0.045
$(\sin\theta/\lambda)_{max}$ (Å^{-1})	0.627	0.830	0.679	0.626	0.628
$R[F^2 > 2\sigma(F^2)]$, $wR(F^2)$, S	0.0310, 0.0871, 1.046	0.0223, 0.0599, 1.031	0.0243, 0.0622, 1.048	0.0326, 0.0999, 1.086	0.0392, 0.1136, 1.032
No. of reflections	12550	28492	14375	12922	12557
No. of parameters	885	818	969	839	843
No. of restraints	470	65	621	37	110
$\Delta\rho_{max}$, $\Delta\rho_{min}$ (e Å^{-3})	0.70, -1.04	1.03, -0.80	0.57, -0.64	0.61, -0.98	1.08, -0.97
Absolute structure parameter	-0.0083(19)	-0.006(3)	-0.019(4)	-0.009(2)	0.010(3)

Computer programs: *CrysAlisPRO*[4] (Rigaku OD, 2020), *SHELXS2013/1*[5] (Sheldrick, 2008) and *SHELXL2018/3*[6] (Sheldrick, 2015).

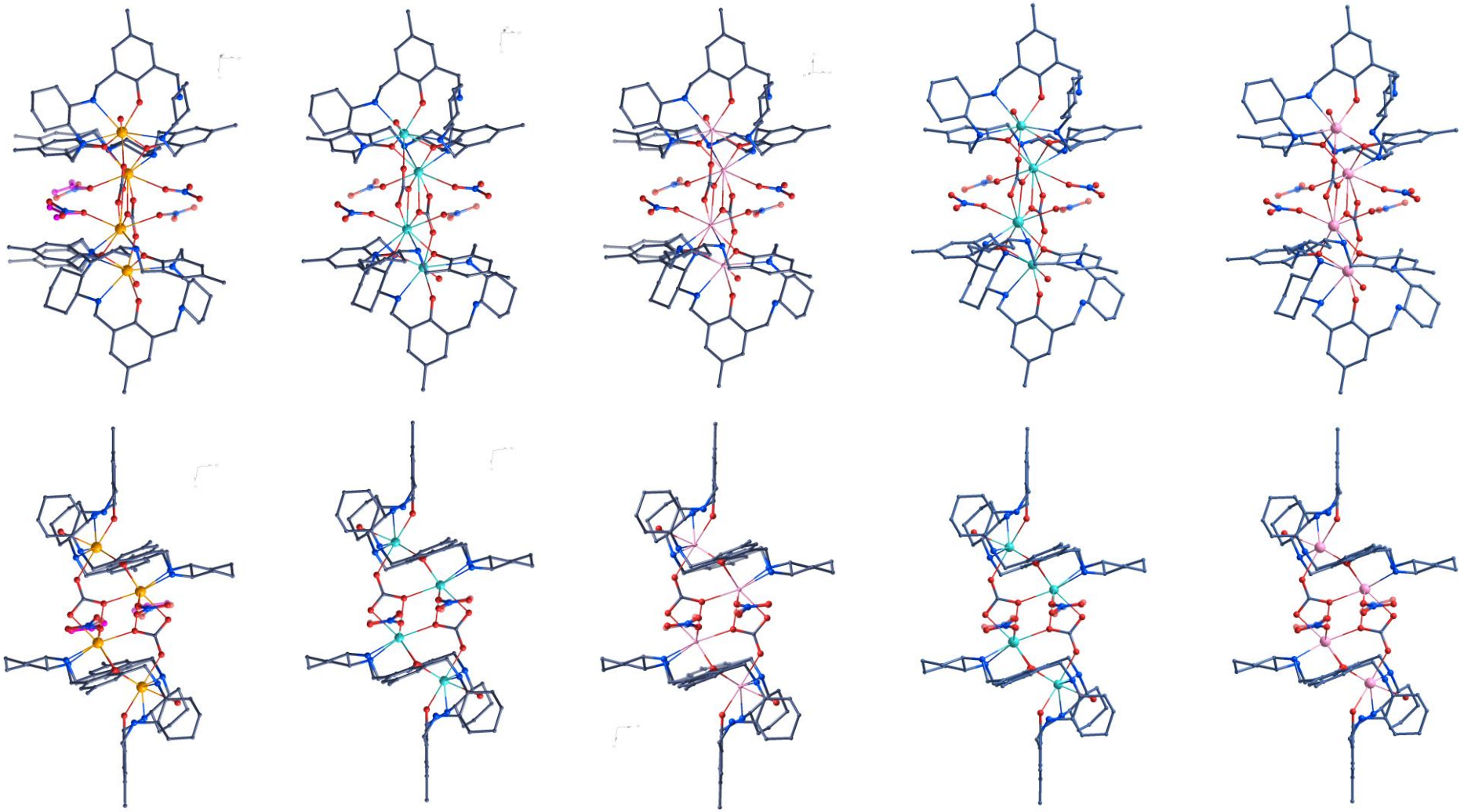

Figure S1 (From left) Side and top view of $[Ln_4(HL^R)_2(CO_3)_2(NO_3)_2(H_2O)_4]^{2+}$ in **1a**, **2a**, **3a**, $\mathbf{2a_{0.5}2a'_{0.5}}$ and $\mathbf{3a_{0.5}3a'_{0.5}}$ respectively. The second disorder components are shown with purple or transparent colours.

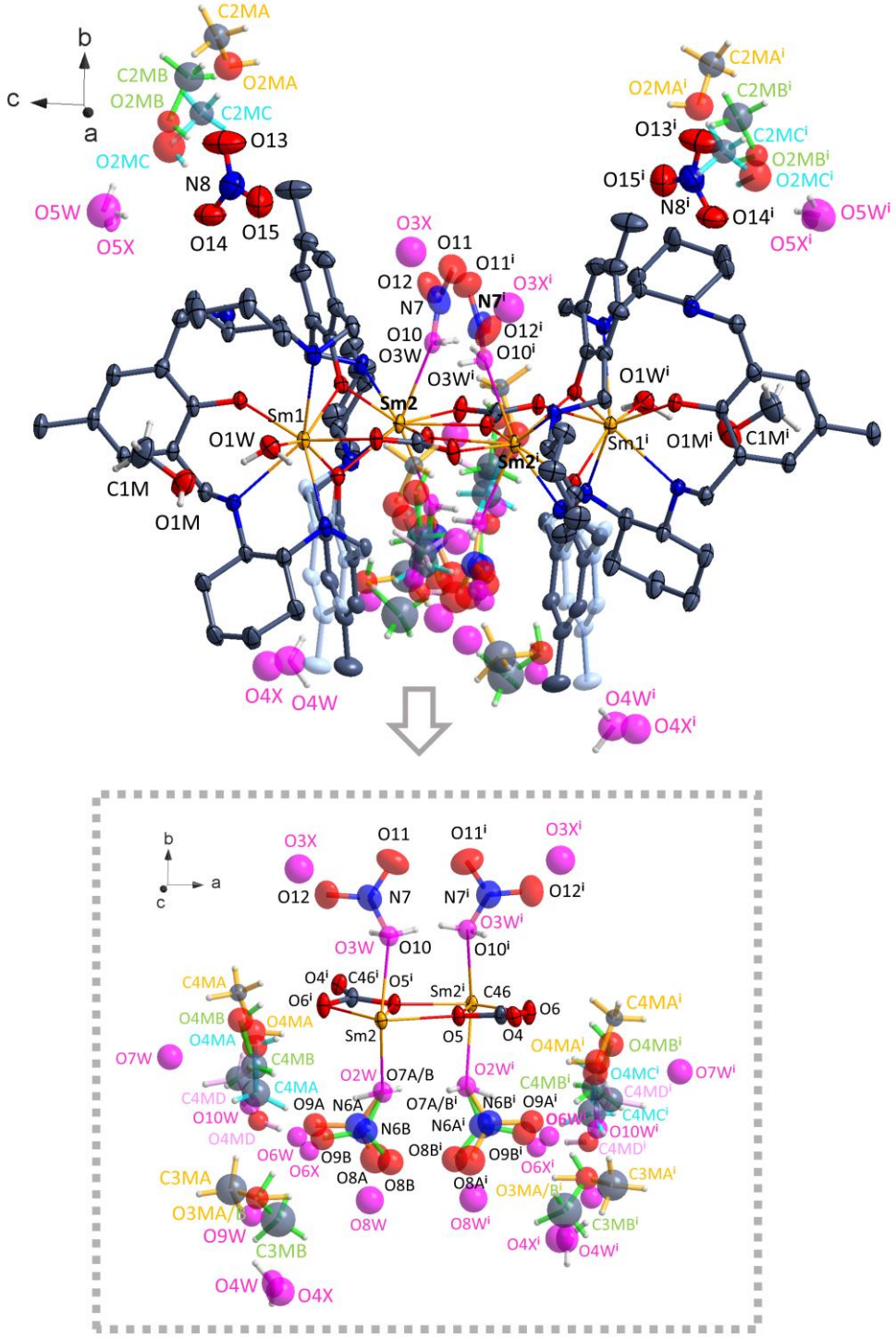

Figure S2 The X-ray structure of $[Sm_4(HL^R)_2(CO_3)_2(NO_3)_2(H_2O)_4](NO_3)_2{\cdot}5.4CH_3OH{\cdot}6H_2O$ (**1a**). For the sake of clarity, the macrocyclic units are shown without atom-numbering scheme, with omitted H-atoms. Colour code: C – dark grey, H – white, N – navy blue, O – red, Sm – yellow. Transparent pink colour represents O-atoms of the partially occupied water molecules. The second disorder component (with SOF = 0.472(17)) of the disordered phenolic fragment in $(HL^R)^{2-}$ is shown in transparent light grey colour. Different positions of the disordered MeOH molecules are represented in different colours. Two positions of disordered nitrates with N6B or N6B^i (symmetry code: (**i**) -*x*+1, *y*, -*z*+1) atoms are shown with green or yellow bonds. The inset reveals the highly disordered solvent/anion region around the Sm2 and Sm2^i ions. Displacement ellipsoids are drawn at the 50% probability level.

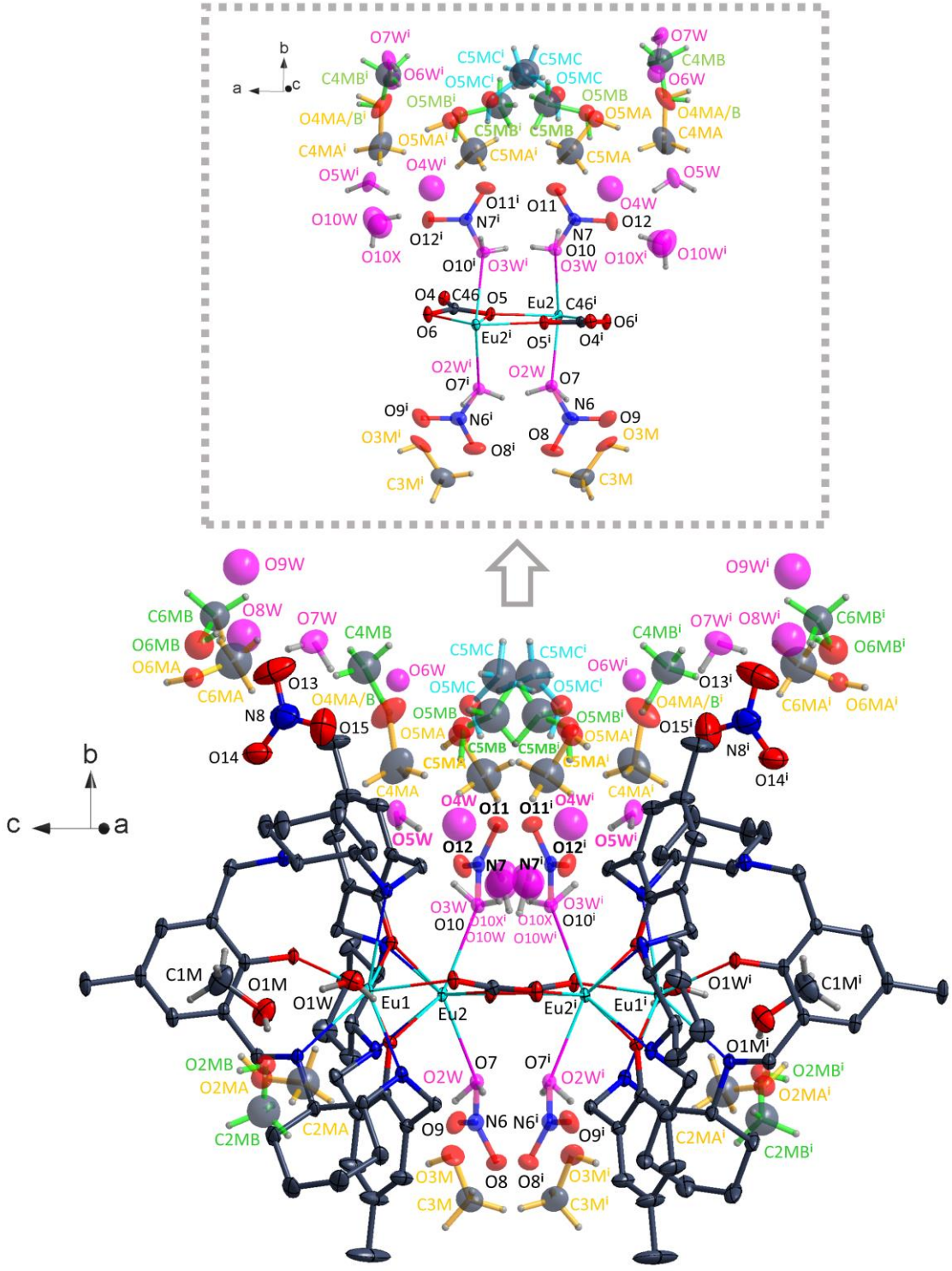

Figure S3 The X-ray structure of $[Eu_4(HL^R)_2(CO_3)_2(NO_3)_2(H_2O)_4](NO_3)_2{\cdot}7.9CH_3OH{\cdot}6H_2O$ (**2a**). For the sake of simplicity, the macrocyclic units are shown without atom-numbering scheme, with omitted H-atoms. Colour code: C – dark grey, H – white, N – navy blue, O – red, Eu – sky blue. Transparent pink colour represents O-atoms of the partially occupied H_2O molecules. Different positions of the disordered MeOH molecules are shown in different colours. Disordered nitrate ions are drawn in transparent colours. The inset reveals the highly disordered solvent/anion region around the Eu2 and Eu2^{i} ions (symmetry code: (**i**) -*x*+1, *y*, -*z*+1). Displacement ellipsoids are drawn at the 50% probability level.

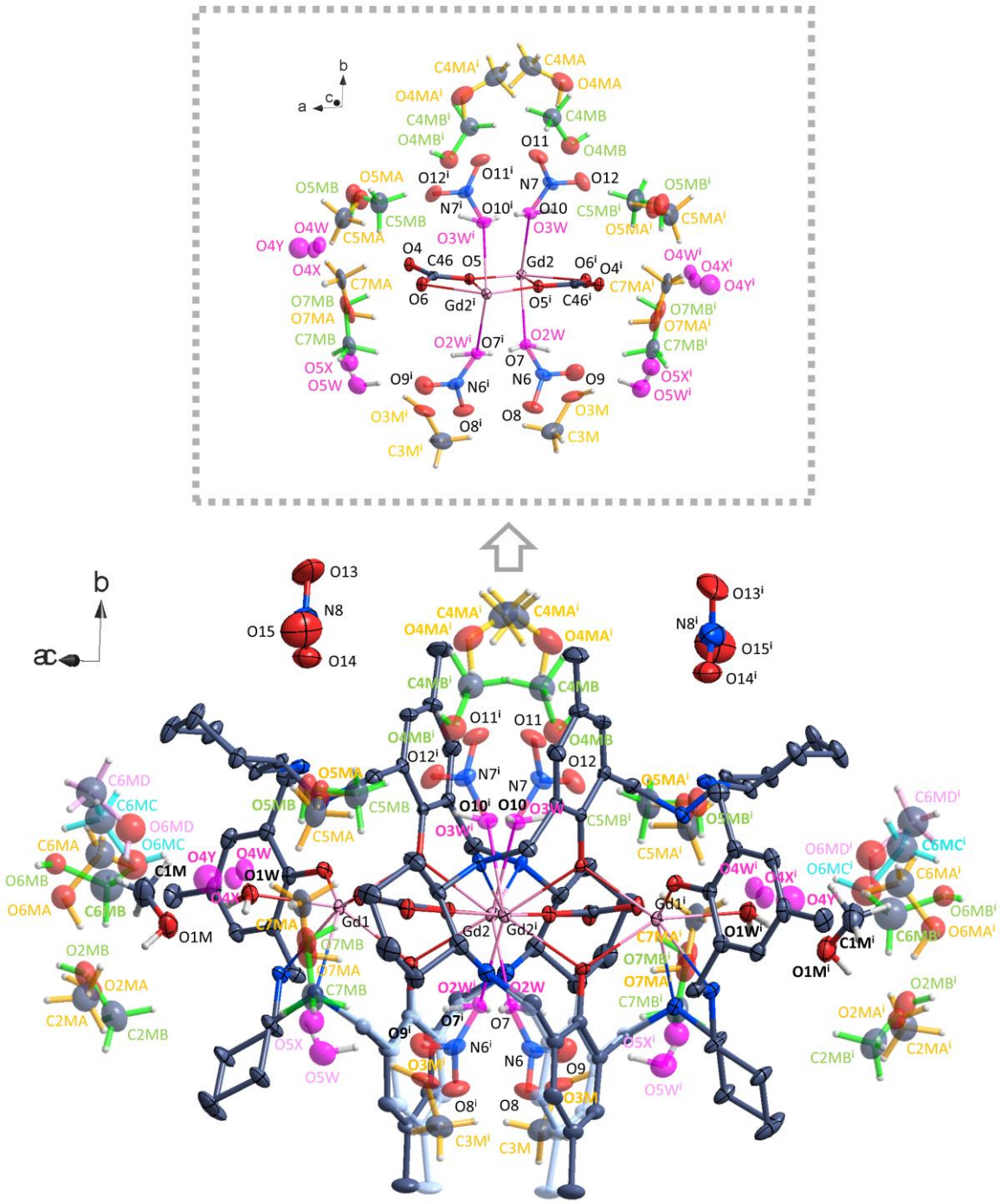

Figure S4 The X-ray structure of $[Gd_4(HL^R)_2(CO_3)_2(NO_3)_2(H_2O)_4](NO_3)_2{\cdot}9.7CH_3OH{\cdot}3.2H_2O$ (**3a**). For the sake of clarity, the macrocyclic units are shown without atom-numbering scheme, with omitted H-atoms. Colour code: C – dark grey, H – white, N – navy blue, O – red, Gd – light pink. Transparent pink colour represents O-atoms of the partially occupied H_2O molecules. The second disorder component of the disordered phenolic fragment in $(HL^R)^{2-}$ (with SOF = 0.37(2)) is shown in transparent light grey colour. Different positions of the disordered MeOH molecules are represented in different colours. Disordered nitrates are shown in transparent colours. The inset reveals the highly disordered solvent/anion region around the Gd2 and Gd2^i ions (symmetry code: (**i**) -*x*+1, *y*, -*z*+1). Displacement ellipsoids are drawn at the 50% probability level.

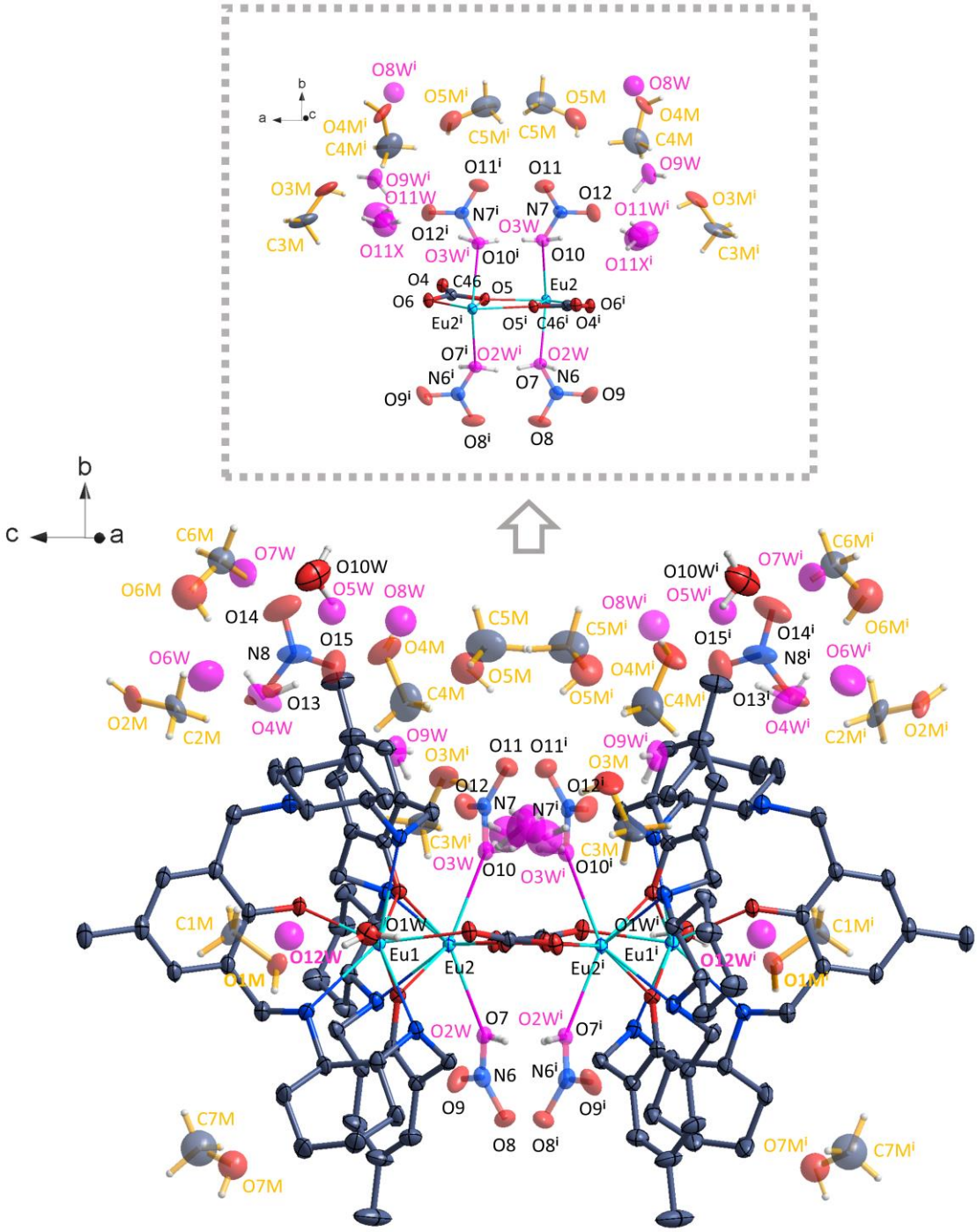

Figure S5 The X-ray structure of $[Eu_4(HL^R)_2(CO_3)_2(NO_3)_2(H_2O)_4]_{0.5}[Eu_4(L^R)_2(CO_3)_2(NO_3)_2(H_2O)_4]_{0.5}(NO_3)\cdot 6.1CH_3OH\cdot 7.7H_2O$ (**2a$_{0.5}$2a'$_{0.5}$**). For the sake of clarity, the macrocyclic units are shown without atom-numbering scheme, with omitted H-atoms. Colour code: C – dark grey, H – white, N – navy blue, O – red, Eu – sky blue. Spheres of transparent pink colour represent O-atoms of the partially occupied H_2O molecules. The partially occupied MeOH molecules are drawn with yellow bonds. The inset shows the highly disordered solvent/anion region around the Eu2 and Eu2^i ions (symmetry code: (**i**) -*x*+1, *y*, -*z*+1). Displacement ellipsoids are shown at the 40% probability level.

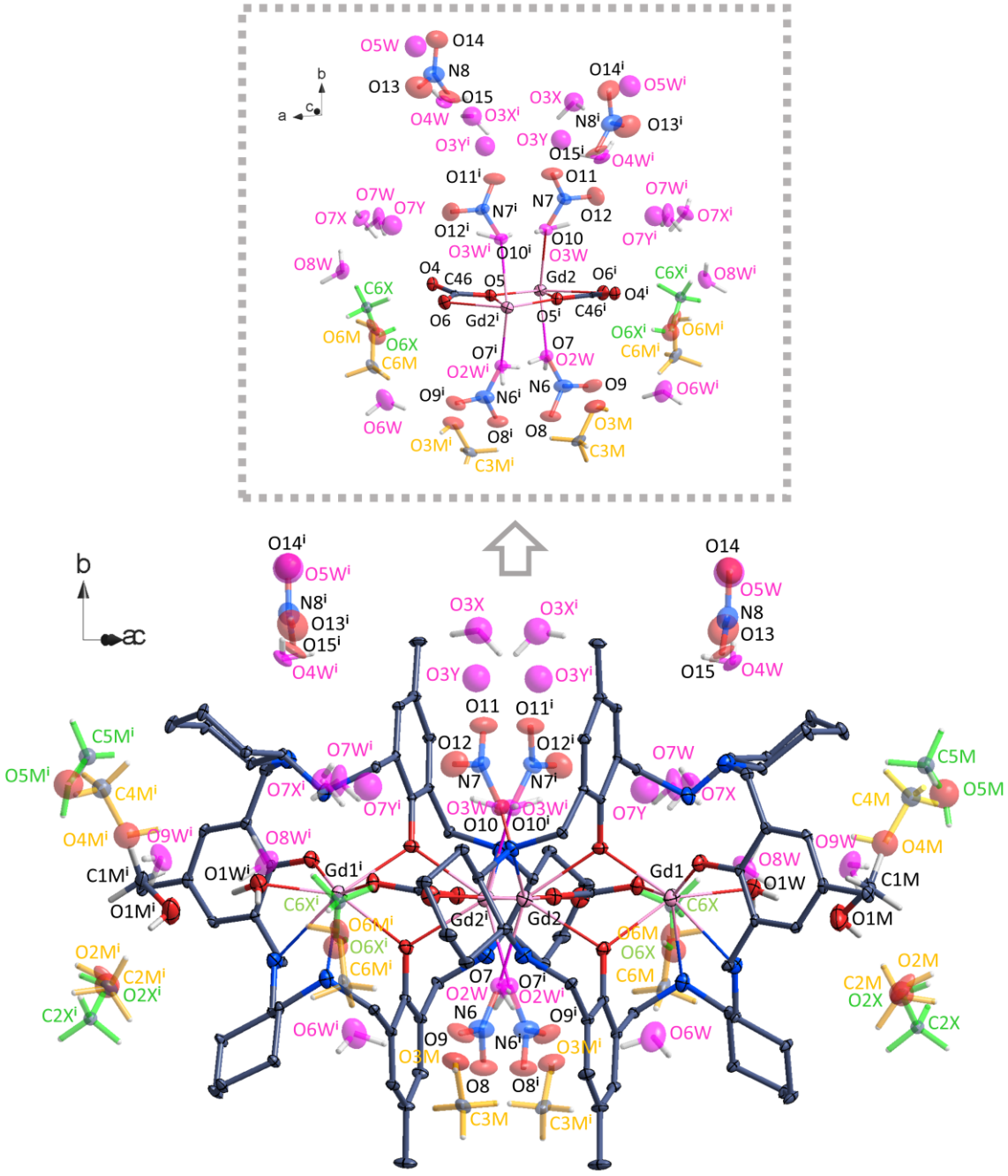

Figure S6 The X-ray structure of $[Gd_4(HL^R)_2(CO_3)_2(NO_3)_2(H_2O)_4]_{0.5}[Gd_4(L^R)_2(CO_3)_2(NO_3)_2(H_2O)_4]_{0.5}(NO_3)\cdot 6.38CH_3OH\cdot 6.7H_2O$ (**3a**$_{0.5}$**3a'**$_{0.5}$). For the sake of clarity, the macrocyclic units are shown without atom-numbering scheme, with omitted H-atoms. Colour code: C – dark grey, H – white, N – navy blue, O – red, Gd – light pink. Transparent pink colour represents O-atoms of the partially occupied H_2O molecules. Different positions of the disordered MeOH molecules are represented in different colours (yellow or green). Disordered nitrates are shown in transparent colours. The inset reveals the highly disordered solvent/anion region around the Gd2 and Gd2^{i} ions (symmetry code: (**i**) *-x*+1, *y*, *-z*+1). Displacement ellipsoids are drawn at the 50% probability level.

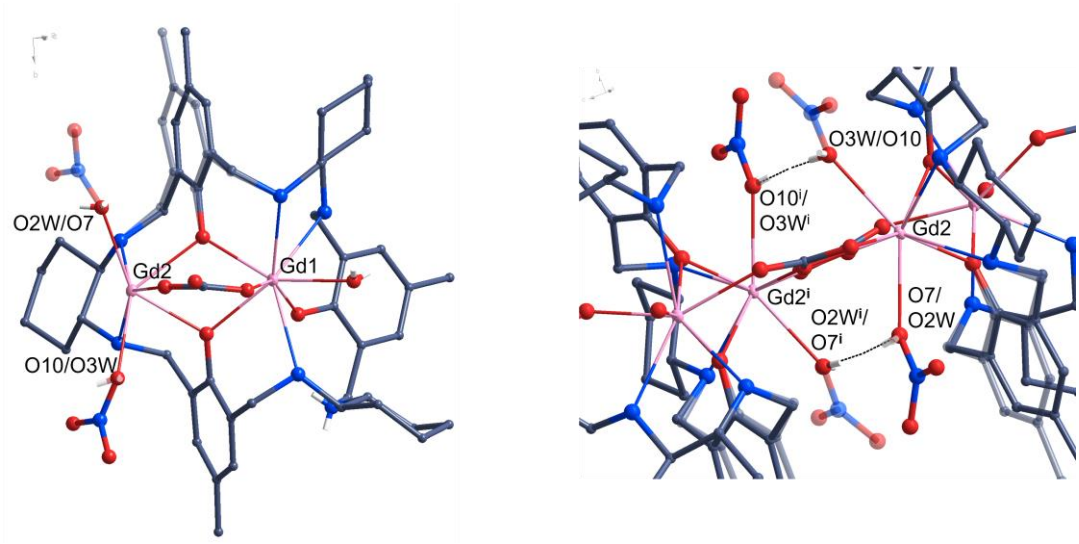

Figure S7 (Left) The asymmetric unit of **3a**. (Right) The disorder of axial positions in **3a**. The free nitrate ion and uncoordinated solvent molecules were omitted for clarity. The second disorder components were shown in transparent colours (symmetry code: -*x*+1, *y*, -*z*+1).

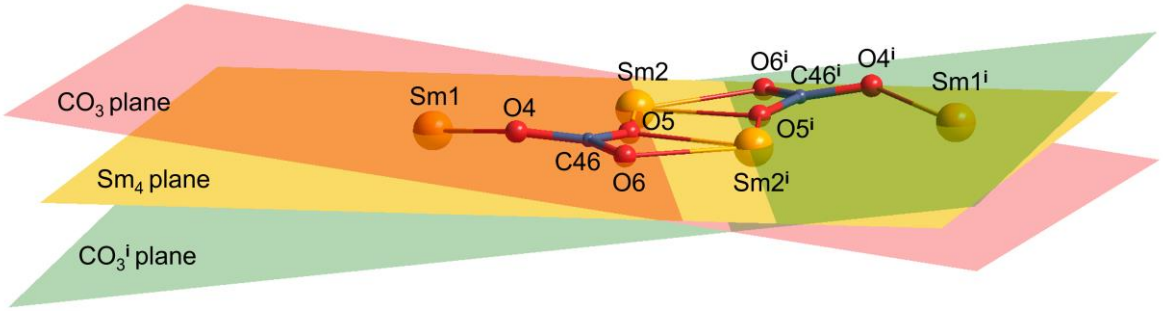

Figure S8 The equivalent dihedral angles formed between Sm_4(Sm1, Sm2, $Sm1^i$, $Sm2^i$) and CO_3(C46, O4, O5, O6) or CO_3^i($C46^i$, $O4^i$, $O5^i$, $O6^i$) planes within the $[Sm_4(CO_3)_2]^{8+}$ cluster in **1a** (symmetry code: (**i**) -*x*+1, *y*, -*z*+1).

Table S2 The internuclear lanthanide···lanthanide distances (Å) and the dihedral angles (°) between planes of Ln_4(*Ln*1, *Ln*2, *Ln*1^{i}, *Ln*2^{i}) and CO_3(O4, O5, O6, C46) or CO_3^{i}(O4^{i}, O5^{i}, O6^{i}, C46^{i}) with their estimated standard deviations for the crystals **1a**-**3a**, **2a$_{0.5}$2a'$_{0.5}$** and **3a$_{0.5}$3a'$_{0.5}$** (symmetry codes: (**i**) -*x*+1, *y*, -*z*+1).

	1a	**2a**	**3a**	**2a$_{0.5}$2a'$_{0.5}$**	**3a$_{0.5}$3a'$_{0.5}$**
*Ln*1···*Ln*2	3.878(1)	3.857(1)	3.841(1)	3.863(1)	3.847(2)
*Ln*1···*Ln*1^{i}	9.157(2)	9.117(2)	9.087(2)	9.136(2)	9.100(3)
*Ln*2···*Ln*2^{i}	4.147(1)	4.146(1)	4.137(1)	4.139(1)	4.125(1)
*Ln*1···*Ln*2^{i}	5.958(1)	5.940(1)	5.924(1)	5.949(1)	5.926(2)
Ln_4/CO_3 or Ln_4/CO_3^{i}	7.86(6)	8.48(3)	8.48(5)	8.85(6)	9.29(7)

Table S3 The coordination bond distances (Å) with their estimated standard deviations for *Ln*1 and *Ln*2 ions in **1a**-**3a**, **2a$_{0.5}$2a'$_{0.5}$** and **3a$_{0.5}$3a'$_{0.5}$** (symmetry code: (**i**) -*x*+1, *y*, -*z*+1).

	1a	**2a**	**3a**	**2a$_{0.5}$2a'$_{0.5}$**	**3a$_{0.5}$3a'$_{0.5}$**
*Ln*1−O1	2.285(4)	2.274(2)	2.271(3)	2.275(4)	2.268(5)
*Ln*1−O2[a]	2.317(4)	2.313(2)	2.299(5)	2.322(4)	2.309(5)
*Ln*1−O3	2.390(4)	2.381(2)	2.368(4)	2.378(4)	2.364(5)
*Ln*1−O4	2.378(4)	2.365(2)	2.358(3)	2.367(3)	2.347(4)
*Ln*1−O1*W*	2.440(4)	2.435(2)	2.420(4)	2.417(4)	2.416(5)
*Ln*1−N1[a]	2.640(5)	2.634(2)	2.618(4)	2.617(5)	2.619(6)
*Ln*1−N4	2.837(5)	2.832(2)	2.826(4)	2.829(5)	2.814(6)
*Ln*1−N9	2.649(5)	2.636(2)	2.627(4)	2.627(5)	2.622(6)
*Ln*2−O2[a]	2.446(4)	2.429(2)	2.429(4)	2.430(4)	2.425(5)
*Ln*2−O3	2.367(4)	2.368(2)	2.353(4)	2.372(4)	2.363(5)
*Ln*2−O5	2.402(3)	2.398(1)	2.390(3)	2.388(3)	2.377(4)
*Ln*2−O5^{i}	2.481(3)	2.477(2)	2.469(3)	2.481(3)	2.471(4)
*Ln*2−O6^{i}	2.460(3)	2.462(2)	2.453(3)	2.466(3)	2.466(4)
*Ln*2−O7/O2W[b]	2.496(5)	2.483(2)	2.466(4)	2.472(4)	2.436(5)
*Ln*2−O10/O3W[b]	2.549(5)	2.540(2)	2.527(4)	2.540(4)	2.540(5)
*Ln*2− N2[a]	2.714(5)	2.707(2)	2.691(5)	2.702(5)	2.697(6)
*Ln*2− N3	2.602(5)	2.598(2)	2.588(5)	2.591(5)	2.585(6)

[a] In **1a** and **3a** atoms O2, N1, and N2 are disordered into two positions O2*A*/O2*B*, N1*A*/N1*B*, and N2*A*/N2*B* with the same coordinates each. Therefore, for these complexes the equal bond distances *Ln*1−O2*A*/*Ln*1−O2*B*, *Ln*2−O2*A*/*Ln*2−O2*B*, *Ln*1−N1*A*/*Ln*1−N1*B*, and *Ln*2−N2*A*/*Ln*2−N2*B* are considered.

[b] The atom pairs O7/O2W or O10/O3W, which are part of substitutionally disordered NO_3^-/H_2O, share the same coordinates and thus the coordination bond distances *Ln*2−O7/*Ln*2−O2W or *Ln*2−O10/*Ln*2−O3W are equal for each O-atom pairs.

Table S4 Continuous Shape Measurements (CShMs)[7] for *Ln*1 and *Ln*2 ions in LnL_8 and LnL_9 fragments, respectively, in crystals **1a**-**3a**, $\mathbf{2a_{0.5}2a'_{0.5}}$ and $\mathbf{3a_{0.5}3a'_{0.5}}$.[a]

	Crystal **1a**	Crystal **2a**	Crystal **3a**	Crystal $\mathbf{2a_{0.5}2a'_{0.5}}$	Crystal $\mathbf{3a_{0.5}3a'_{0.5}}$
Ideal structures for LnL_8[b]	Sm1	Eu1	Gd1	Eu1	Gd1
SAPR-8 (D_{4d})	5.031	4.930	4.888	4.925	4.908
TDD-8 (D_{2d})	3.269	3.208	3.178	3.174	3.138
JBTP-8 (C_{2v})	2.707	2.695	2.669	2.704	2.638
BTPR-8 (C_{2v})	3.517	3.476	3.455	3.476	3.464
JSD-8 (D_{2d})	**1.938**	**1.918**	**1.895**	**1.911**	**1.892**
Ideal structures for LnL_9[c]	Sm2[d]	Eu2[d]	Gd2[d]	Eu2[d]	Gd2[d]
JCSAPR-9 (C_{4v})	3.272	3.158	3.177	3.148	3.130
CSAPR-9 (C_{4v})	**1.983**	**1.963**	**1.985**	**1.992**	**2.010**
JTCTPR-9 (D_{3h})	5.016	4.919	4.936	4.873	4.878
TCTPR-9 (D_{3h})	2.785	2.835	2.843	2.832	2.860
MFF-9 (C_s)	2.371	2.342	2.358	2.339	2.358

[a] Only those with the smallest deviations from the ideal structures are given.

[b] Ideal reference polyhedra for LnL_8:
SAPR-8 – Square antiprism
TDD-8 – Triangular dodecahedron
JBTP-8 – Johnson - Biaugmented trigonal prism (J50)
BTPR-8 – Biaugmented trigonal prism
JSD-8 – Snub disphenoid (J84)

[c] Ideal reference polyhedra for LnL_9:
JCSAPR-9 – Capped square antiprism (Gyroelongated square pyramid J10)
CSAPR-9 – Capped square antiprism
JTCTPR-9 – Tricapped trigonal prism (J51)
TCTPR-9 – Tricapped trigonal prism
MFF-9 – Muffin

[d] The donor O-atoms of substitutionally disordered H_2O and NO_3^- share the same coordinates.

3. Powder X-ray diffraction

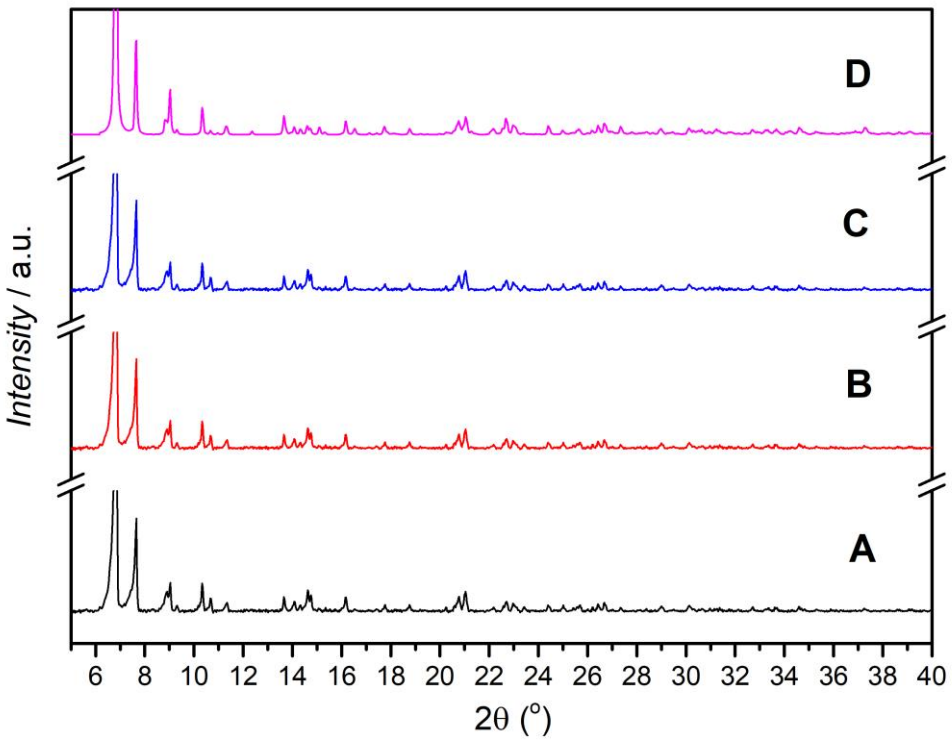

Figure S9 The experimental PXRD patterns for complexes (A) **1a**, (B) **3a** and (C) **2a** compared with PXRD pattern for (D) **2a** simulated from single-crystal X-ray data.

4. IR spectra

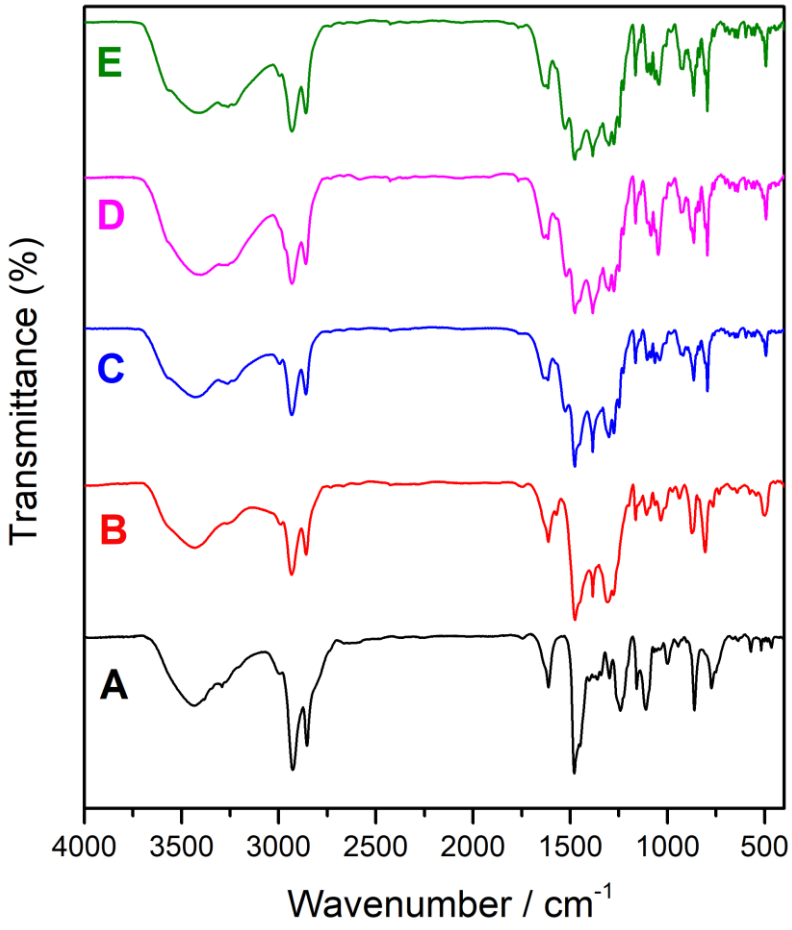

Figure S10 Comparison of IR spectra of the macrocycle $H_3\mathbf{L}^{R}$ (**A**) and the nitrate complex $[Eu(H_2\mathbf{L}^{R})(NO_3)_2]$[1] (**B**) with those of the carbonate complexes $[Ln_4(H\mathbf{L}^{R})_2(CO_3)_2(NO_3)_2(H_2O)_4](NO_3)_2$ (Ln^{III} = Eu^{III} for **2a** (**C**), Sm^{III} for **1a** (**D**), and Gd^{III} for **3a** (**E**)).

5. NMR spectrum of the ligand H_3L^R

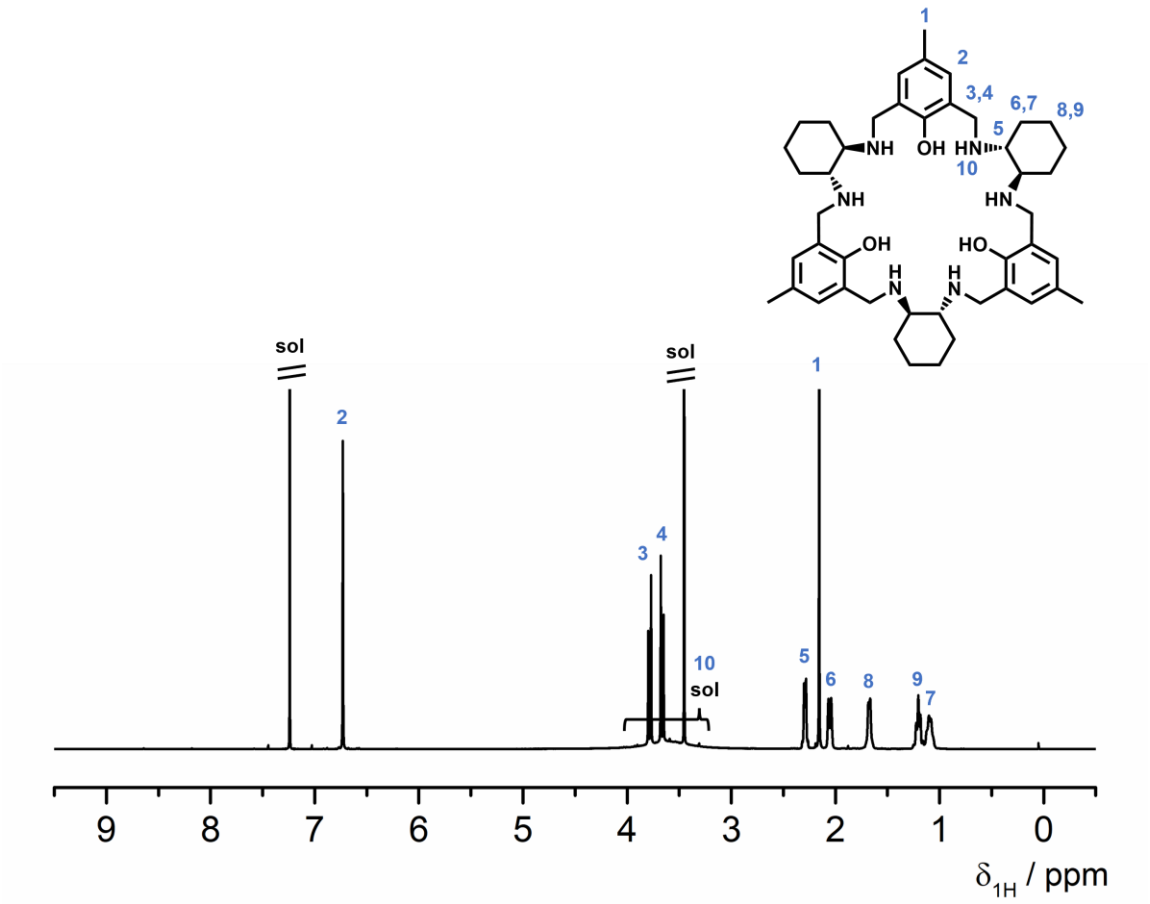

Figure S11 The ^{1}H NMR spectrum (500 MHz, 300 K) of ligand H_3L^R in dried $CDCl_3$.[1-3]

6. NMR spectra of complex 2a

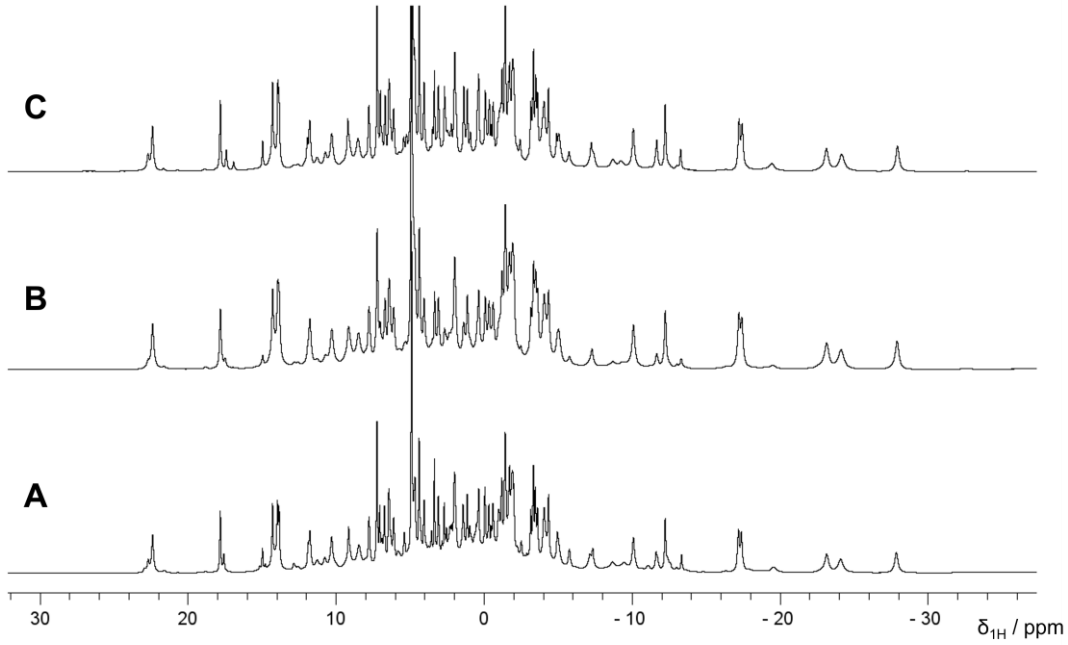

Figure S12 The ^{1}H NMR spectra of **2a** (CD_3OD/D_2O 20:1, [**2a**]$_0$ =4.4 mM, 500 MHz, 300 K) synthesized using different molar ratios of $Eu(NO_3)_3$, $H_3\mathbf{L}^{R}$, K_2CO_3 and TMAH: (A) 1.9:1:0.5:1.9, (B) 2:1:0.5:2 and (C) 2:1:1:2.

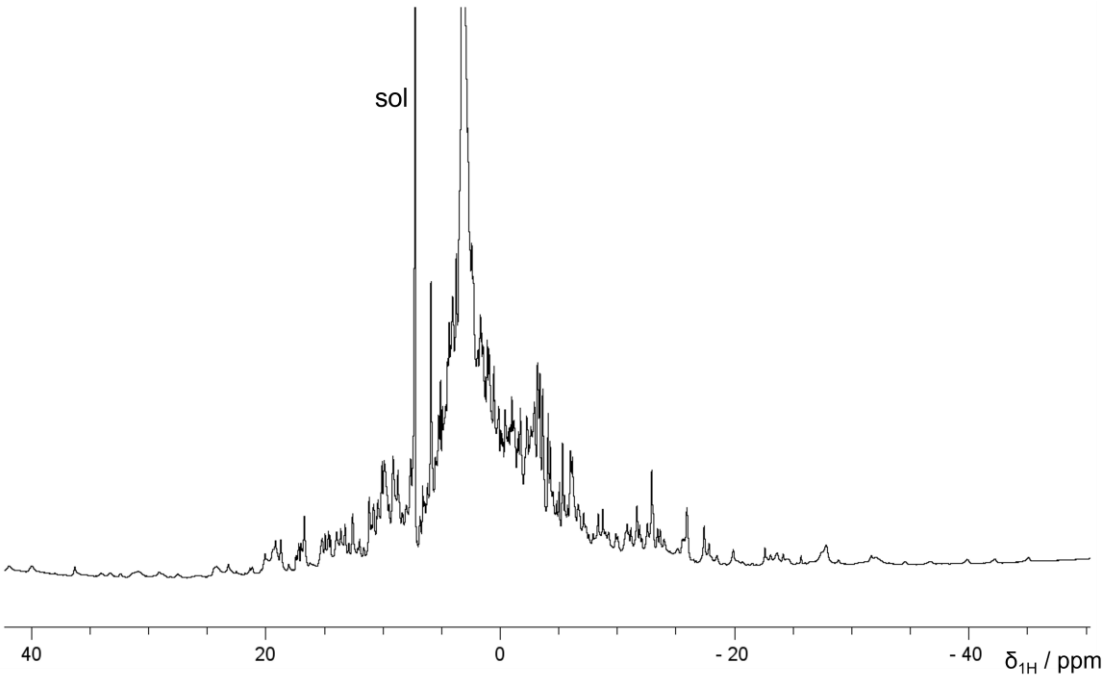

Figure S13 The ^{1}H NMR spectrum of **2a** in dried $CDCl_3$ (500 MHz, [**2a**]$_0$ = 4.0 mM, 300 K). Sol denote signal of the solvent.

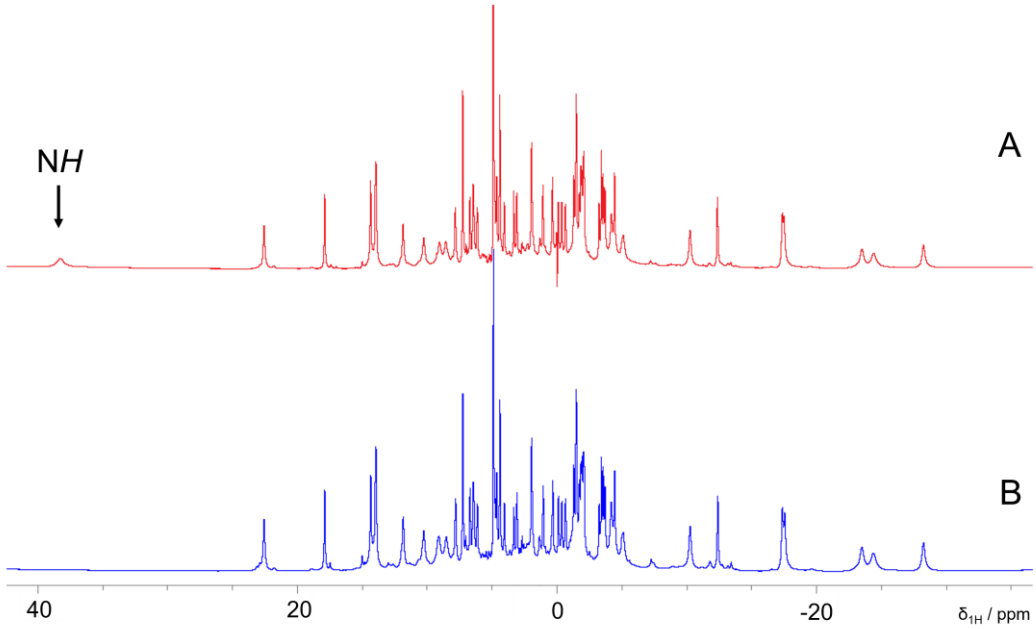

Figure S14 (**A**) The ^{1}H NMR spectrum (CD_3OD/D_2O 20:1, [**2a**] = 7.1 mM, 600 MHz, 300 K) of $[Eu_4(HL^R)_2(CO_3)_2(NO_3)_2(H_2O)_4](NO_3)_2$ (**2a**) recorded immediately after dissolution of the sample. The NH signal was indicated by arrow. (**B**) The ^{1}H NMR spectrum (CD_3OD/D_2O 20:1, [**2a**] = 7.1 mM, 600 MHz, 300 K) of deuterated form of **2a**, $[Eu_4(DL^R)_2(CO_3)_2(NO_3)_2(D_2O)_4](NO_3)_2$, measured immediately after dissolution of the sample. The deuterated form of the complex was synthesized by first dissolving the free macrocycle H_3L^R in CD_3OD/D_2O solvent mixture to ensure that all NH and OH positions become ND and OD positions and then repeating the reaction of complex formation.

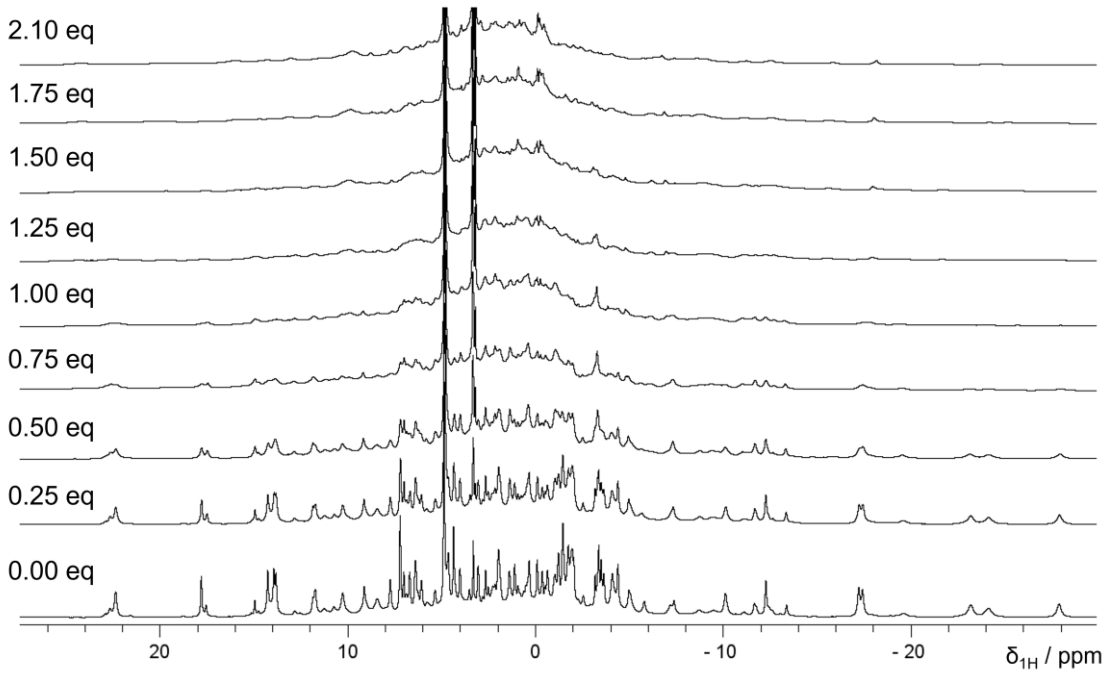

Figure S15 The ^{1}H NMR spectra recorded during titration of **2a** (CD_3OD/D_2O 20:1 (v/v) solution, $[\mathbf{2a}]_0$ = 4.4 mM, 500 MHz, 300 K) with TMAH.

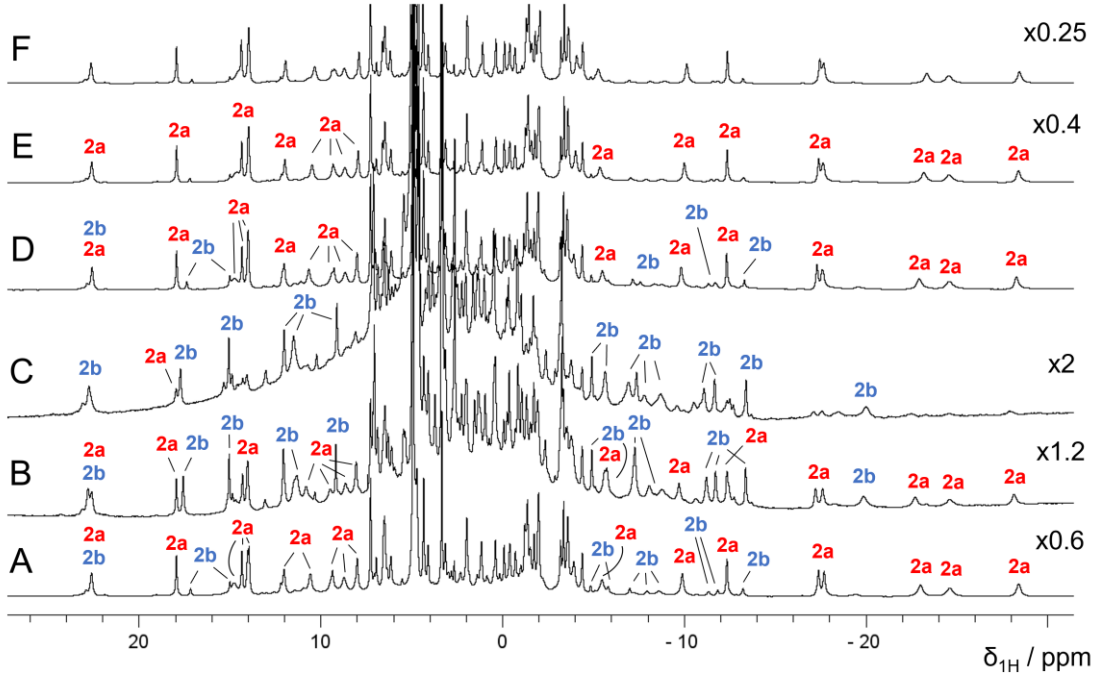

Fig. S16 (A) The ^{1}H NMR spectrum (CD_3OD/D_2O 20:1 v/v, [**2a**]$_0$ = 3.0 mM, 500 MHz, 300 K) of **2a**. The ^{1}H NMR spectra of the solution recorded after (B) 4-fold ([**2a**]$_0$ = 0.8 mM), (C) 8-fold ([**2a**]$_0$ = 0.4 mM) dilution and total addition of (D) 3 mg ([**2a**]$_0$ = 2.2 mM), (E) 8 mg ([**2a**]$_0$ = 5.2 mM), and (F) 13 mg ([**2a**]$_0$ = 8.2 mM) of the sample. Some of the down- and upshifted signals of the complexes **2a** and **2b** were denoted with red and blue colours, respectively.

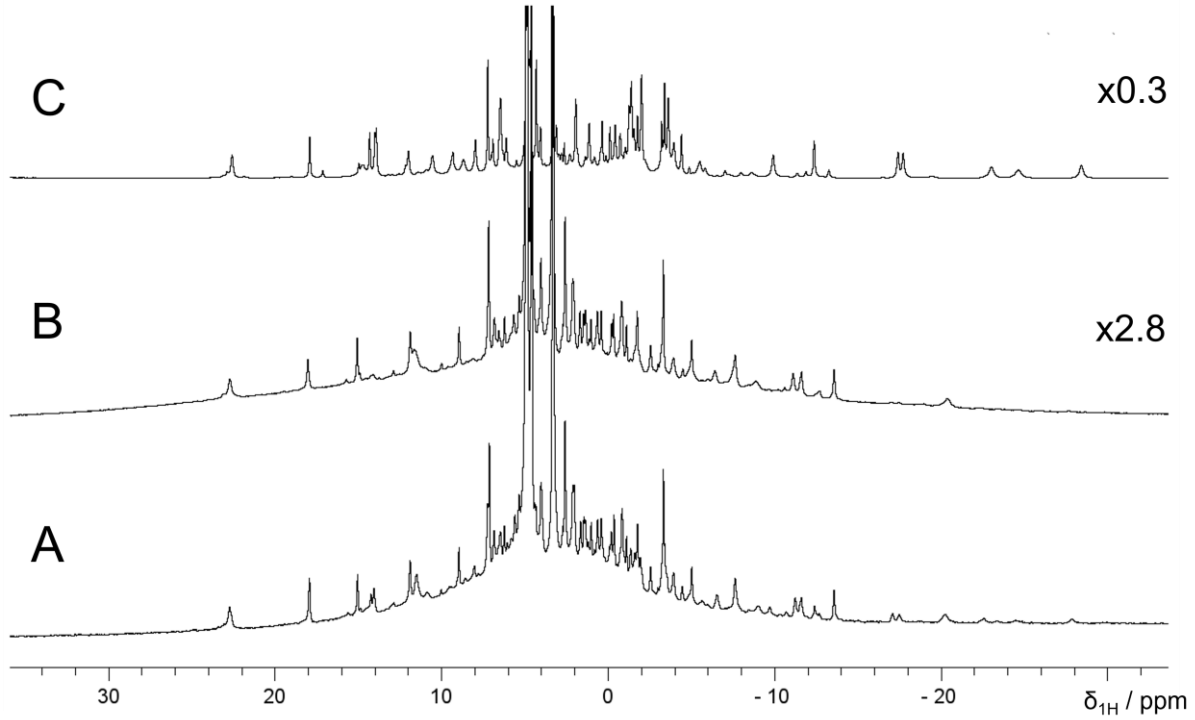

Figure S17 The ^{1}H NMR spectra of **2a** (CD_3OD/D_2O 20:1 (v/v), 500 MHz, 300 K) at the concentration of (A) 0.3 mM and (C) 3.0 mM. (B) The ^{1}H NMR spectrum obtained by dissolving of 10 crystals of **2a** in 430 µl of CD_3OD/D_2O 20:1 (v/v) solvent mixture.

7. ESI-MS spectra

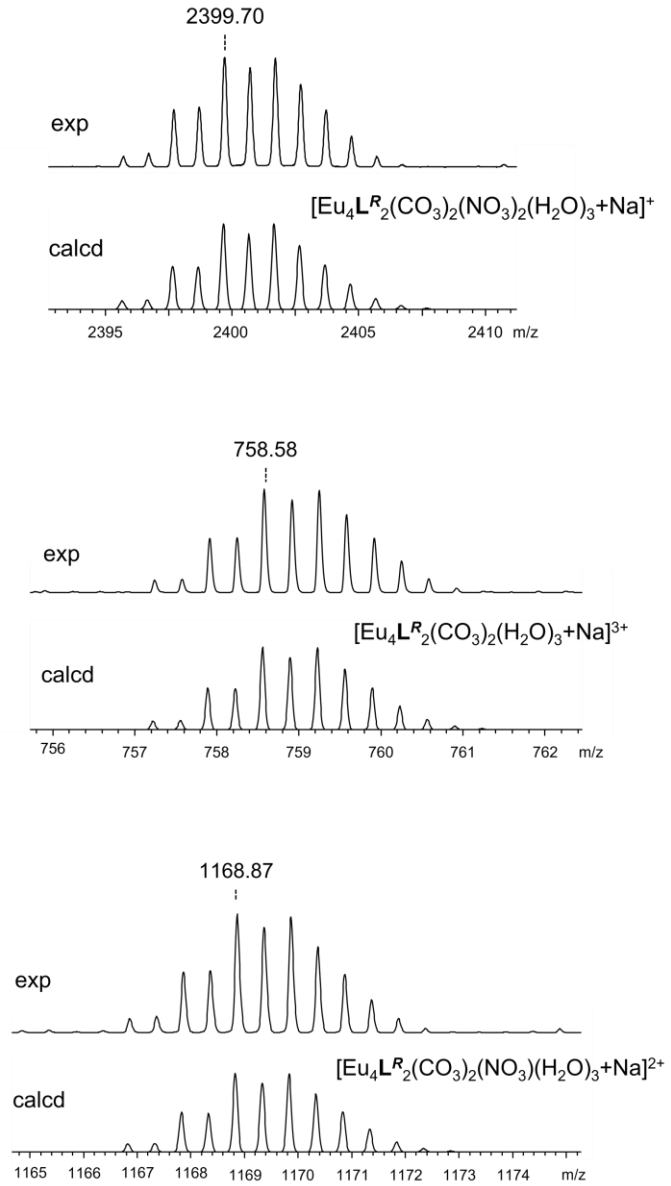

Figure S18 Experimental and theoretical isotope patterns for various tetranuclear coordination cations derived from **2a**.

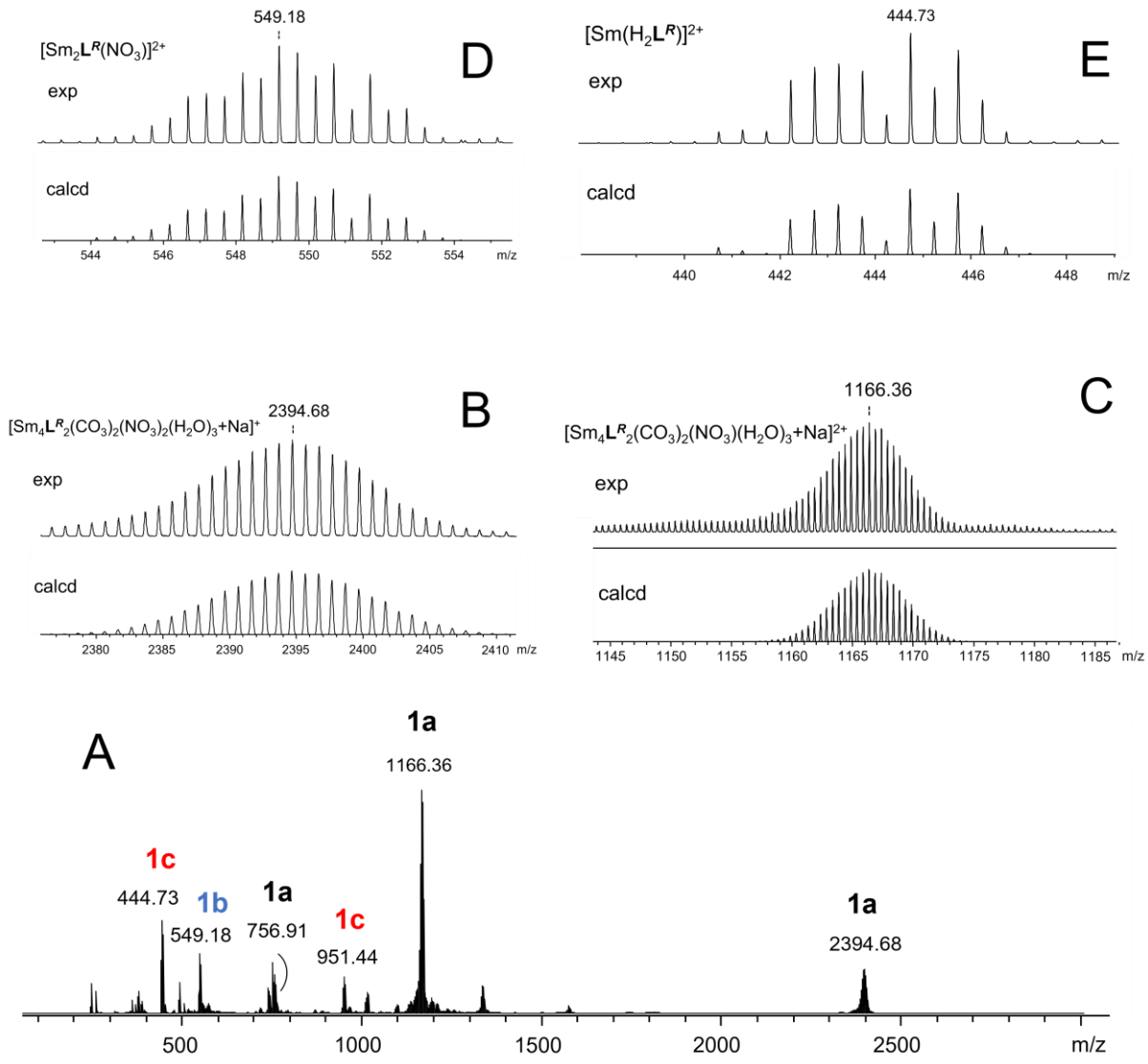

Figure S19 (A) The ESI-MS spectrum of the **1a**/**1b**/**1c** mixture obtained upon dissolving **1a** in methanol. The insets show comparison of experimental and theoretical isotope patterns for various coordination cations derived from **1a** (B, C), **1b** (D) and **1c** (E).

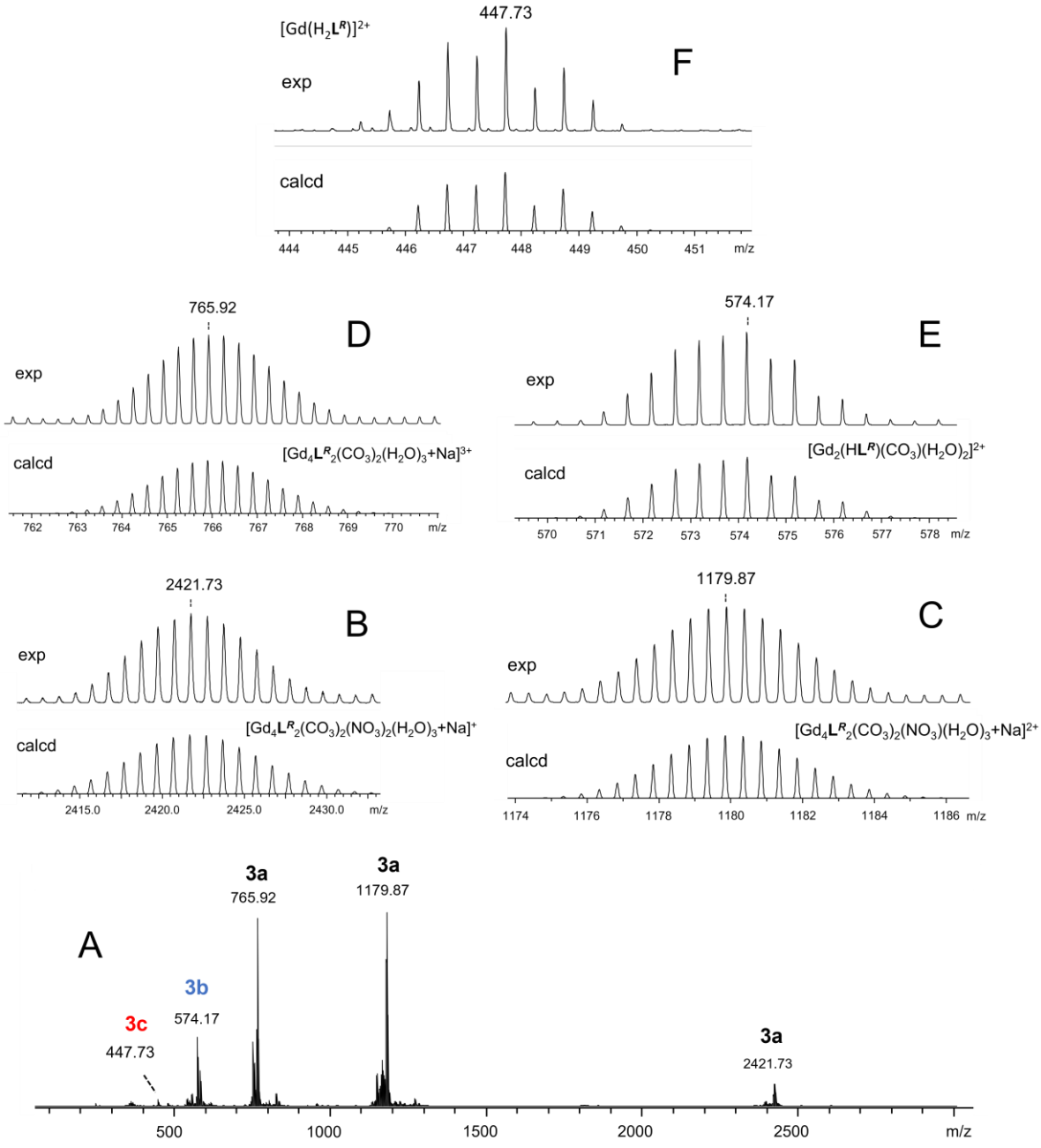

Figure S20 (A) The ESI-MS spectrum of the **3a**/**3b**/**3c** mixture obtained upon dissolving of **3a** in methanol. The insets show comparison of experimental and theoretical isotope patterns for various coordination cations derived from **3a** (B, C, and D), **3b** (E) and **3c** (F).

8. NMR spectra of complex 1a and the signals assignment

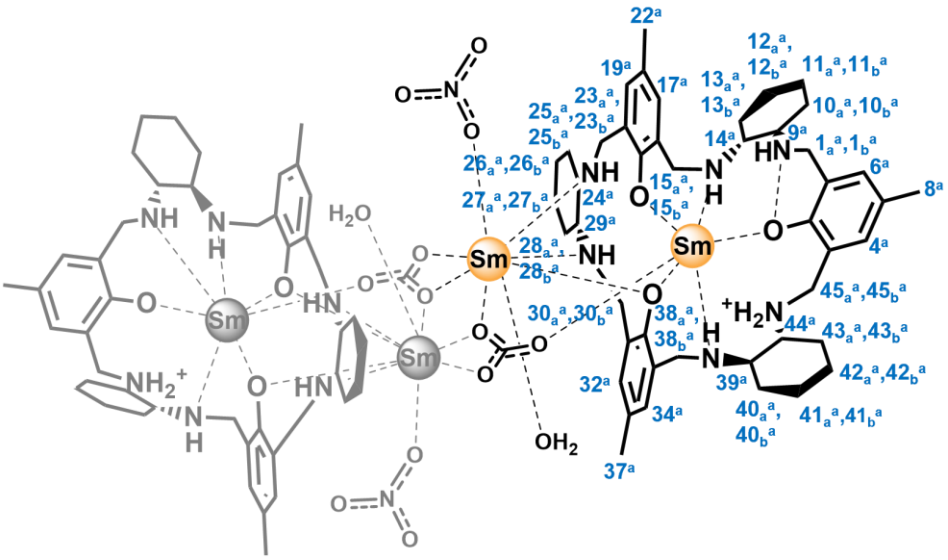

Scheme S2 Labelling scheme for H-atoms of the macrocycle $(HL^{R})^{2-}$ in complex **1a**.

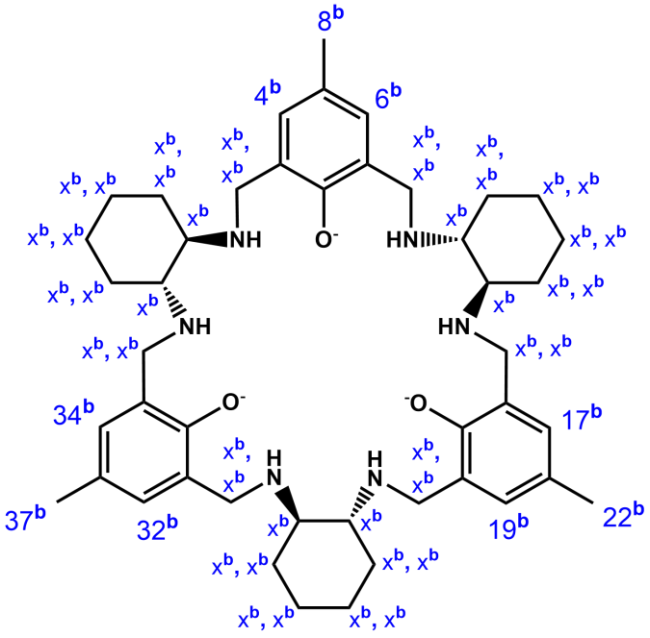

Scheme S3 Labelling scheme for H-atoms of the macrocycle $(HL^{R})^{2-}$ in coordination form **1b**.

Assignment of the ^{1}H NMR signals of complex 1a

The ^{1}H NMR signals of **1a** are overlapped, especially in the aliphatic region. Thus, some of the expected correlations were not observed on the measured 2D spectra. The assignment starts with three narrow singlets with 6H intensity at 2.62, 1.03 and 1.40 ppm, which correspond to three sets of methyl protons 8^{a}, 22^{a} and 37^{a}, respectively (see Fig. 6 in main text; Scheme S2). The ^{13}C NMR signals of corresponding methyl C-atoms $C_{8}{}^{a}$, $C_{22}{}^{a}$, and $C_{37}{}^{a}$ were identified on the basis of strong HSQC correlations (Fig. S34, Scheme S4). The HSQC spectrum also indicate the presence of six signals of different phenyl protons (Fig. S35). These signals can be easily assigned to three proton pairs 4^{a}+6^{a}, 17^{a}+19^{a}, and 32^{a}+34^{a} of each aromatic ring, on the basis of COSY correlations (Fig. S21). Followingly, the connectivity between signals of phenyl and methyl protons was inferred from ROESY and NOESY correlations (Fig. S25 and S30). The HSQC spectrum confirmed the presence of six different methylene bridges. The assignment of the geminal protons $1_{a}{}^{a}$+$1_{b}{}^{a}$, $15_{a}{}^{a}$+$15_{b}{}^{a}$, $23_{a}{}^{a}$+$23_{b}{}^{a}$, $30_{a}{}^{a}$+$30_{b}{}^{a}$, $38_{a}{}^{a}$+$38_{b}{}^{a}$, and $45_{a}{}^{a}$+$45_{b}{}^{a}$ was further substantiated by strong ROESY, NOESY or COSY cross-peaks (Fig. S21, S25 and S30). Subsequently, one of the signals of each proton pair is NOESY and/or ROESY correlated to one signal of phenyl protons. As a matter of fact, the correlations between signals 6^{a}+$1_{a}{}^{a}$, 4^{a}+$45_{b}{}^{a}$, 17^{a}+$15_{a}{}^{a}$, 19^{a}+$23_{b}{}^{a}$, 32^{a}+$30_{a}{}^{a}$, and 34^{a}+$38_{a}{}^{a}$ were observed. The HSQC spectrum allows for convenient identification of the six signals of cyclohexane methine protons 9^{a}, 14^{a}, 24^{a}, 29^{a}, 39^{a}, and 44^{a}. In fact, each of the signals is correlated to only one signal of corresponding C-atom: $C_{9}{}^{a}$, $C_{14}{}^{a}$, $C_{23}{}^{a}$, $C_{29}{}^{a}$, $C_{39}{}^{a}$, and $C_{44}{}^{a}$.

In general, there are three types of cyclohexane fragments in the macrocyclic unit $(H\mathbf{L}^{\boldsymbol{R}})^{2-}$ of the complex. These three spin systems comprise 10 signals of aliphatic protons each. The identification of signals of first cyclohexane ring starts with the NOESY and ROESY correlations between signal 39^{a} of methine proton and signals $38_{a}{}^{a}$ and 34^{a} of methylene bridge and phenyl protons, respectively. The signal 39^{a} also give rise to three strong COSY cross-peaks with signals 44^{a}, $40_{a}{}^{a}$ and $40_{b}{}^{a}$ (Fig. S22). The first signal belong to methine proton, while the other two have to correspond to geminal protons. Subsequently, the signal $40_{a}{}^{a}$ is COSY correlated to the signals $41_{a}{}^{a}$ and $41_{b}{}^{a}$ of neighbouring geminal proton pair. Geminal signals of the third consecutive proton pair were identified on the basis of COSY, NOESY or ROESY correlations $41_{a}{}^{a}$+$42_{b}{}^{a}$, $41_{b}{}^{a}$+$42_{a}{}^{a}$, and $41_{b}{}^{a}$+$42_{b}{}^{a}$ (Fig. S26-S28, 32 and 33). These two signals are in turn COSY correlated to signals $43_{a}{}^{a}$ and $43_{b}{}^{a}$ of the last geminal proton pair. The assignment of the first cyclohexane ring is completed by COSY, NOESY and ROESY correlations of signals $43_{b}{}^{a}$ and 44^{a}. The resonances of the geminal protons were additionally identified on the basis of HSQC correlations (Fig. S36). These protons are also ROESY, NOESY and COSY correlated. Some of the expected ROESY and NOESY cross-peaks between vicinal protons were not observed (this was also found for other cyclohexane spin systems of **1a**). The final proof for the assignment was provided by TOCSY correlations of proton $40_{a}{}^{a}$ with remaining 9 protons of given spin system (Fig. S24).

The assignment for the second cyclohexane fragment starts with up-field shifted signal 24^a of methine proton, appearing at -0.42 ppm. The resonance is COSY correlated to three signals, one of which is the signal 29^a of other methine proton, hence remaining two signals have to correspond to geminal protons $25_a{}^a$ and $25_b{}^a$. Another three geminal proton pairs $26_a{}^a$+$26_b{}^a$, $27_a{}^a$+$27_b{}^a$, and $28_a{}^a$+$28_b{}^a$ were identified sequentially on the basis of COSY, NOESY, and ROESY cross-peaks. The COSY correlations between geminal protons $28_a{}^a$+$28_b{}^a$ and methine proton 29^a are also observed. The final confirmation of the assignment was provided by HSQC and TOCSY data.

Two remaining resonances 9^a and 14^a of methine protons appearing at 4.47 ppm and 8.71 ppm, respectively, have to correspond to the third (and last) cyclohexane ring. The TOCSY correlations of the signal 14^a show that the eight signals of geminal protons are highly overlapped (Fig. S24). Thus, only tentative signal assignment of given spin system was possible The COSY spectrum identifies correlations between proton 9^a and protons 14^a, $10_a{}^a$, and $10_b{}^a$ (Fig. S21). In addition, the NOE cross-peak is observed between signals 9^a and $10_a{}^a$. Subsequently, the signal $10_b{}^a$ is COSY, NOESY and ROESY correlated to the signal $11_a{}^a$ of second geminal proton pair (Fig. S22, S26-S28 and S32). After careful inspection of the HSQC correlations between geminal protons it become apparent that the resonance $11_b{}^a$ exhibits the same chemical shift (δ = 2.35 ppm) as the resonance $10_a{}^a$ (Fig S36). This resulted in the absences of $10_a{}^a$+$11_b{}^a$ cross-peak and overlapping of the correlations $10_a{}^a$+$10_b{}^a$ and $10_b{}^a$+$11_b{}^a$, as well as $10_a{}^a$+$11_a{}^a$ and $11_a{}^a$+$11_b{}^a$. The assignment is continued by COSY cross-peaks $11_a{}^a$+$12_a{}^a$ (δ = 2.54 ppm) and $11_b{}^a$+$12_a{}^a$. The remaining geminal signal $12_b{}^a$ of third proton pair was identified based on HSQC and COSY correlations. Subsequently, the signal $12_a{}^a$ is COSY correlated to the signal $13_b{}^a$ of last geminal proton pair. This signal, in turn, give rise to COSY correlation with the resonance 14^a of methine proton. The COSY and HSQC correlations between geminal protons $13_a{}^a$ and $13_b{}^a$ are also observed on the spectra. A further connectivity of given spin system is provided only by the NOE and ROE contact between proton $11_a{}^a$ with phenyl proton 17^a.

The connectivity between the spin systems of the macrocyclic subunits $(H\mathbf{L}^{\boldsymbol{R}})^{2-}$ in the complex is provided by ROE and NOE cross-peaks: $45_b{}^a$+$43_a{}^a$, $38_a{}^a$+39^a, 34^a+39^a, $28_a{}^a$+$30_a{}^a$, and 17^a+$11_a{}^a$. These correlations are in accord with the X-ray crystal structure of **1a** (see Fig. 6B in main discussion), which confirms that the conformation of the macrocycle $(H\mathbf{L}^{\boldsymbol{R}})^{2-}$ in the complex is preserved in the solution. The interatomic distances between abovementioned protons, based on the crystal structure of **1a**, are as followed: 2.29, 2.18, 2.68, 2.22 and 3.72 Å. These connectives allows for preliminary assignment of 51 signals corresponding to C-H protons of the complex, although some of the expected NOESY and ROESY correlations are missing (e.g., $23_b{}^a$+24^a and $1_a{}^a$+$10_a{}^a$). (The protons $1_a{}^a$, $1_b{}^a$, 4^a, 6^a, 8^a, 9^a, $10_a{}^a$, $10_b{}^a$, 14^a, $15_a{}^a$, $15_b{}^a$, 17^a, 19^a, 22^a, $23_a{}^a$, $23_b{}^a$, 24^a, $28_a{}^a$, $28_b{}^a$, 29^a, $30_a{}^a$, $30_b{}^a$, 32^a, 34^a, 37^a, $38_a{}^a$, $38_b{}^a$, 39^a, $43_a{}^a$, $43_b{}^a$, 44^a, $45_a{}^a$, and $45_b{}^a$ were numbered in the same manner as in the crystal structure of the complex. The remaining cyclohexane protons were labelled with arbitrary chosen subscripts).

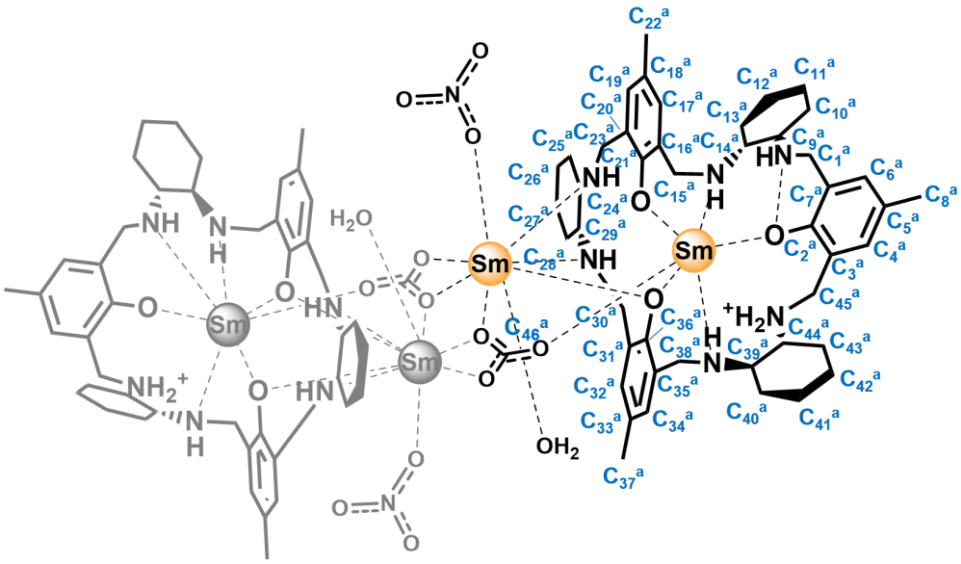

Scheme S4 Labelling scheme for C-atoms of the macrocycle $(HL^{R})^{2-}$ in complex **1a**.

Assignment of the ^{13}C NMR signals of complex 1a

33 out of 46 ^{13}C NMR signals of complex **1a** correspond to carbon atoms with bonded hydrogen atoms. These signals were identified based on HSQC spectrum (Fig. S34-S36). Some of the remaining 12 ^{13}C signals of phenyl C-atoms were assigned with the aid of HSQC and HMBC data. Three down-shifted signals, resonating at 171.16, 153.89, and 162.74 ppm, correspond to C_2^a, C_{21}^a, and C_{36}^a C-atoms, respectively, which are directly attached to an electronegative hydroxyl oxygen atom (Fig. S34 and S37). Subsequently, each of the three resonances at 126.32, 124.65, and 126.23 ppm exhibit no HSQC cross-peaks and only one HMBC two-bond correlation to methyl protons (Fig. S37-S39). Thus, the signals have to correspond to C_5^a, C_{18}^a, and C_{33}^a carbon atoms, respectively. The signal of C_3^a atom was identified on the basis of HMBC two-bond correlations: C_3^a+45_a^a and C_3^a+45_b^a. The remaining five signals of phenyl C-atoms attached to methylene bridges were not assigned, since these signals exhibit no HMBC cross-peaks (the unassigned signals were denoted as C_x^a on the ^{13}C NMR spectra). The resonances appear at 119.12, 125.36, 126.23, 128.11, and 131.04 ppm, which are typical positions for phenyl carbon atoms. The last ^{13}C signal of **1a**, which is highly downshifted (δ = 190.48 ppm) and exhibit no HMBC and HSQC correlations, corresponds to the carbon atom C_{46}^a of carbonate anion (see main discussion).

Assignment of the ^{1}H NMR signals of complex form 1c

The spectral pattern of the coordination form **1c**, which is observed in the trace amounts on the ^{1}H NMR spectrum of **1a**, is consistent with the effective C_2 symmetry in solution. Accordingly, three phenyl signals of the same intensity belonging to **1c** were found at 7.72, 7.37, and 7.13 ppm, while two methyl peaks - the first one of 6H and the second of 3H intensity - appear at 2.54 and 2.31 ppm, respectively. Notably, the NOESY spectrum (as well as the ROESY spectrum recorded at 330 K, see Fig. S25-S29, S43 and S44) showed the

exchange-type correlations between resonances of phenyl or methyl protons. This indicates a migration of the metal ion within the macrocyclic cavity, which constitute a characteristic feature of the mononuclear rare earth(III) complexes of $H_3\mathbf{L}^{\boldsymbol{R}}$.[1,8] The monometallic $Sm(H_x\mathbf{L}^{\boldsymbol{R}})(NO_3)_x$ ($0 \le x \le 4$) structure of **1c** is in accordance wit the ESI-MS spectrum obtained upon dissolving of **1a** in methanol (see main discussion and Fig. S19).

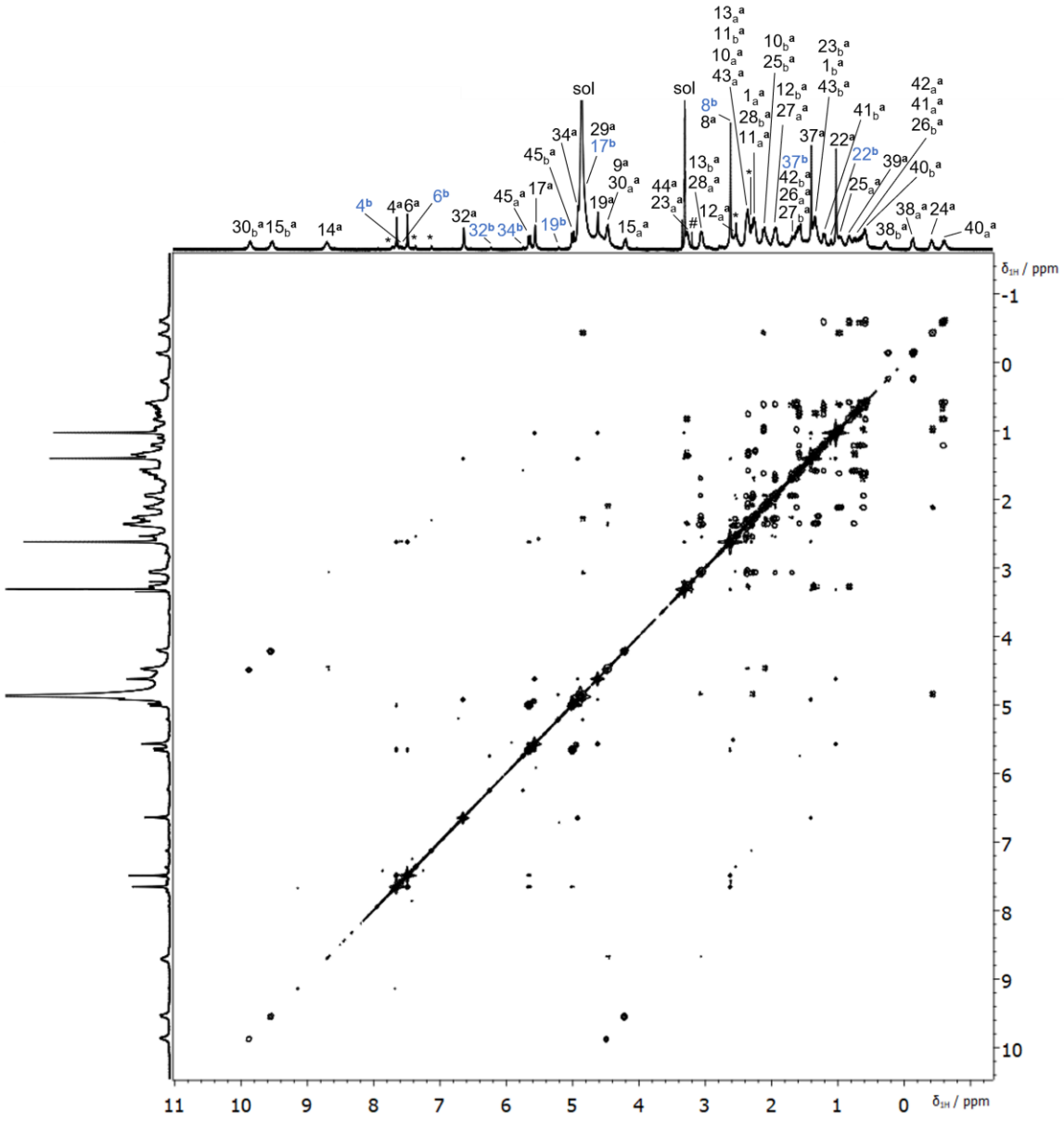

Figure S21 The COSY spectrum (500 MHz, 300 K) obtained upon dissolving of **1a** in CD_3OD/D_2O 20:1 (v/v) mixture ($[\mathbf{1a}]_0$ = 16.5 mM). The signals of coordination species **1a**, **1b**, and **1c** were labeled with a superscript "a", "b" or by an asterisk, respectively. Octothorpe denote signals of the impurities; signals sol of solvents.

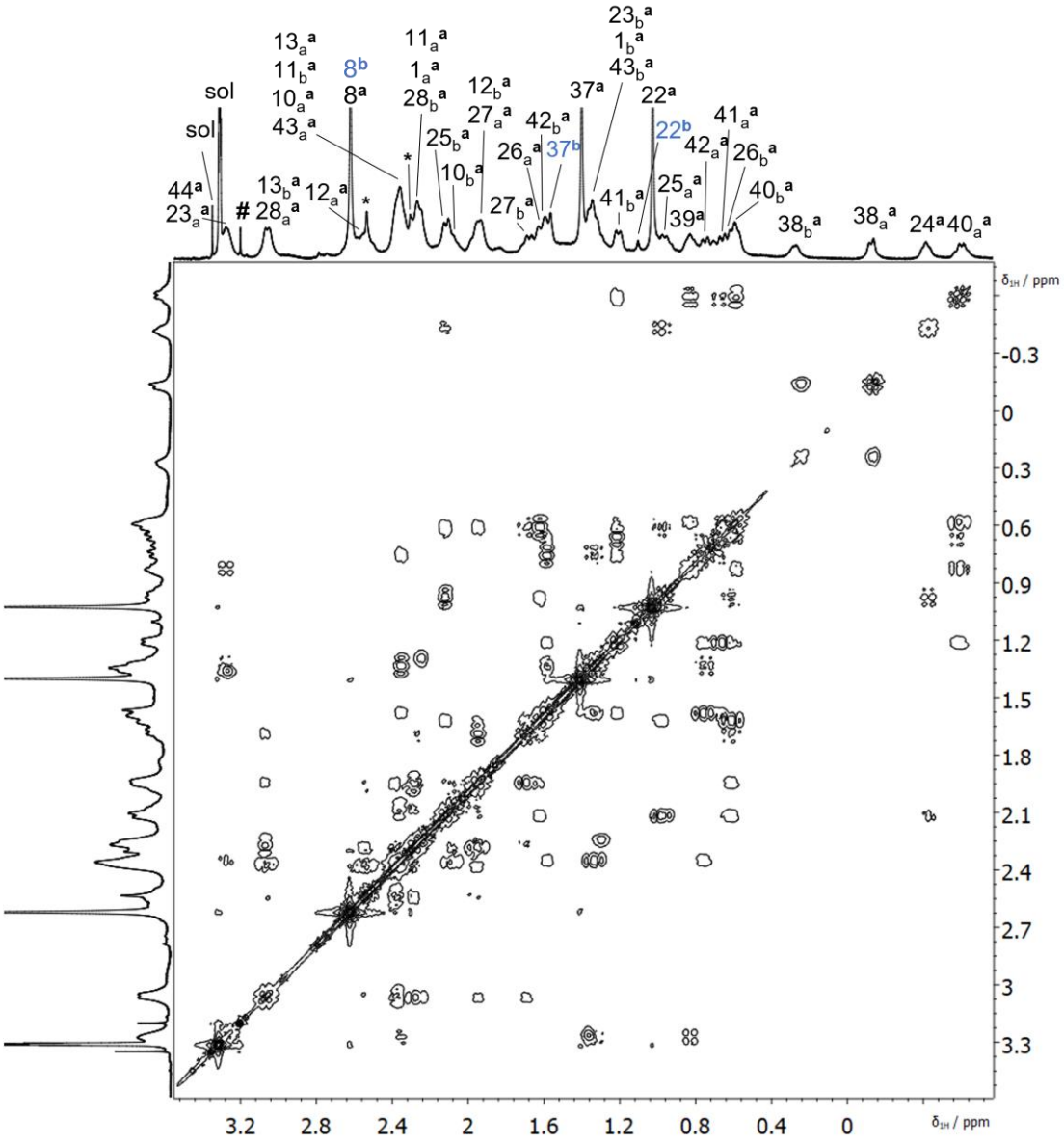

Figure S22 Aliphatic part of the COSY spectrum (500 MHz, 300 K) obtained upon dissolving of **1a** in CD_3OD/D_2O 20:1 (v/v) mixture ($[\mathbf{1a}]_0$ = 16.5 mM). The signals of coordination species **1a**, **1b**, and **1c** were labeled with a superscript "a", "b" or by an asterisk, respectively. Octothorpe denote signals of the impurities; signals sol of solvents.

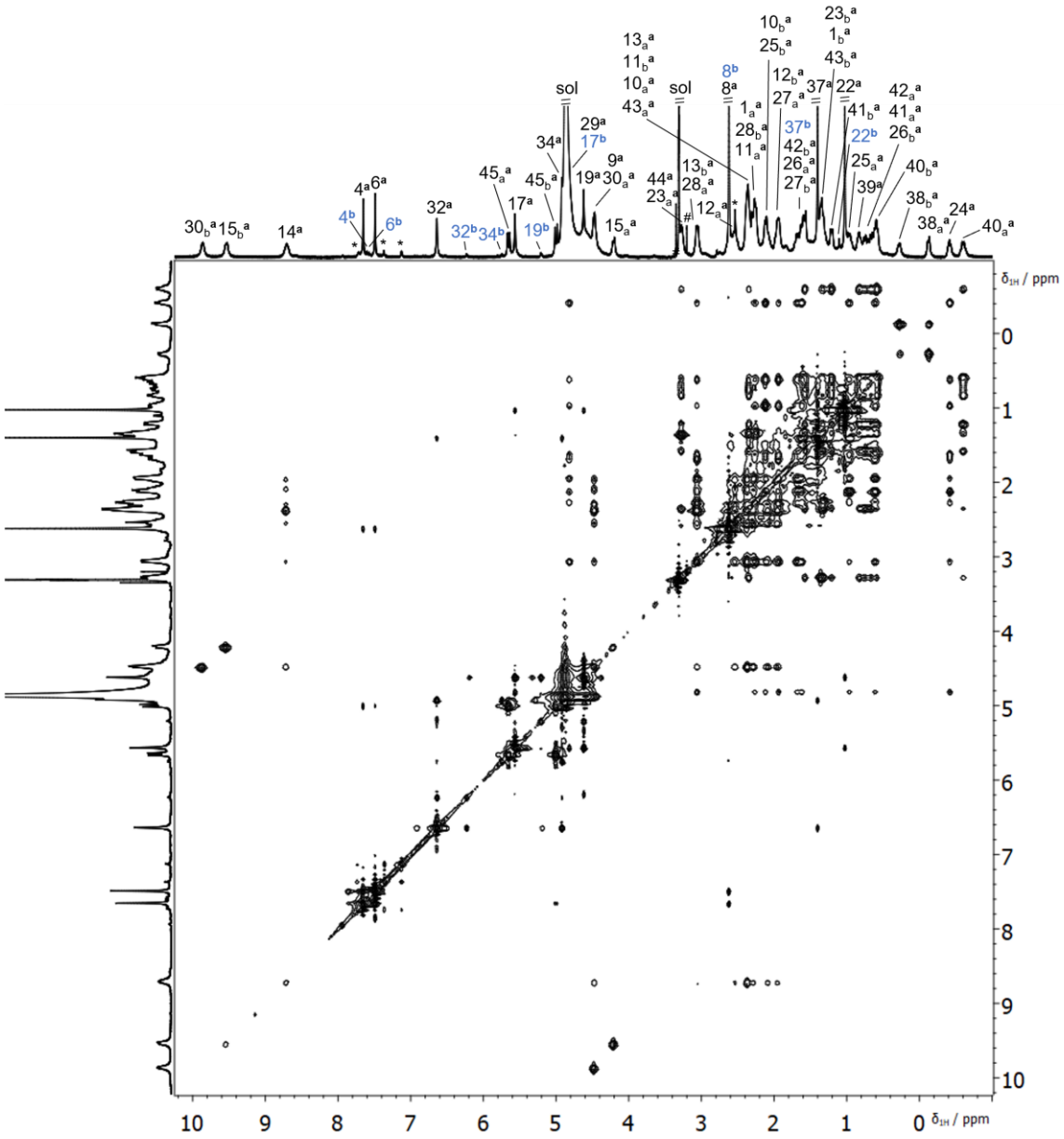

Figure S23 The TOCSY spectrum (500 MHz, 300 K) obtained upon dissolving of **1a** in CD_3OD/D_2O 20:1 (v/v) mixture ($[\mathbf{1a}]_0$ = 16.5 mM). The signals of coordination species **1a**, **1b**, and **1c** were labeled with a superscript "a", "b" or by an asterisk, respectively. Octothorpe denote signals of the impurities; signals sol of solvents.

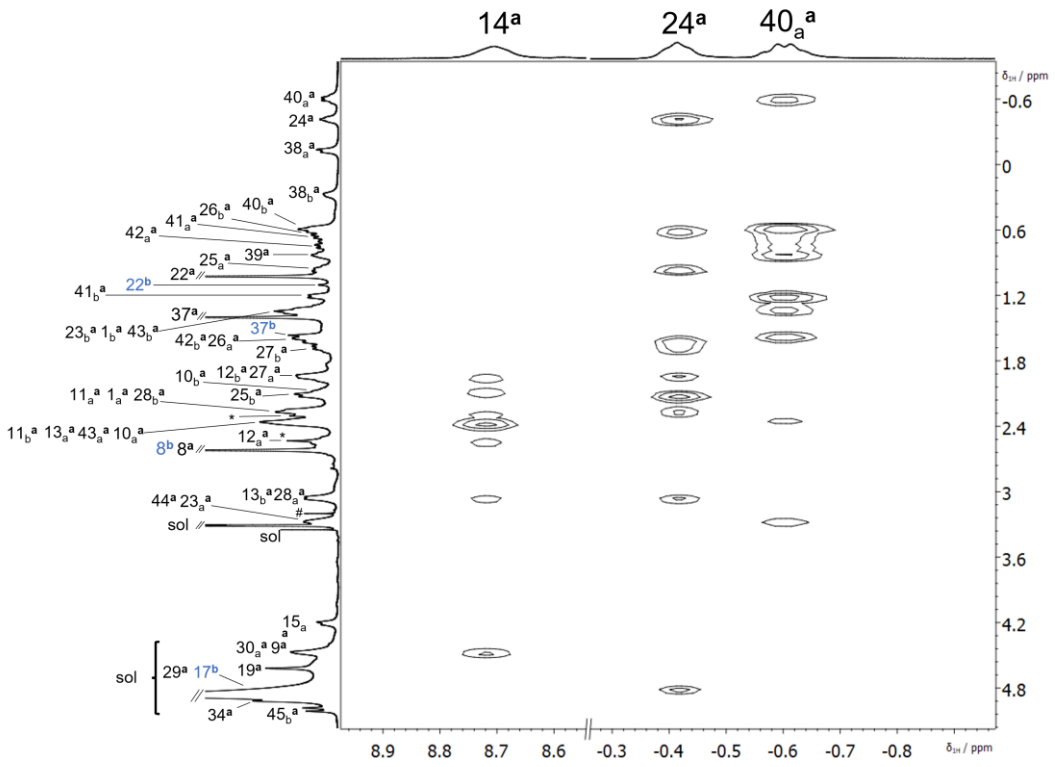

Figure S24 Part of the TOCSY spectrum (500 MHz, 300 K) obtained upon dissolving of **1a** in CD_3OD/D_2O 20:1 (v/v) mixture ($[\mathbf{1a}]_0$ = 16.5 mM), showing correlations between signals of three cyclohexane spin systems. The signals of coordination species **1a**, **1b**, and **1c** were labeled with a superscript "a", "b" or by an asterisk, respectively. Octothorpe denote signals of the impurities; signals sol of solvents.

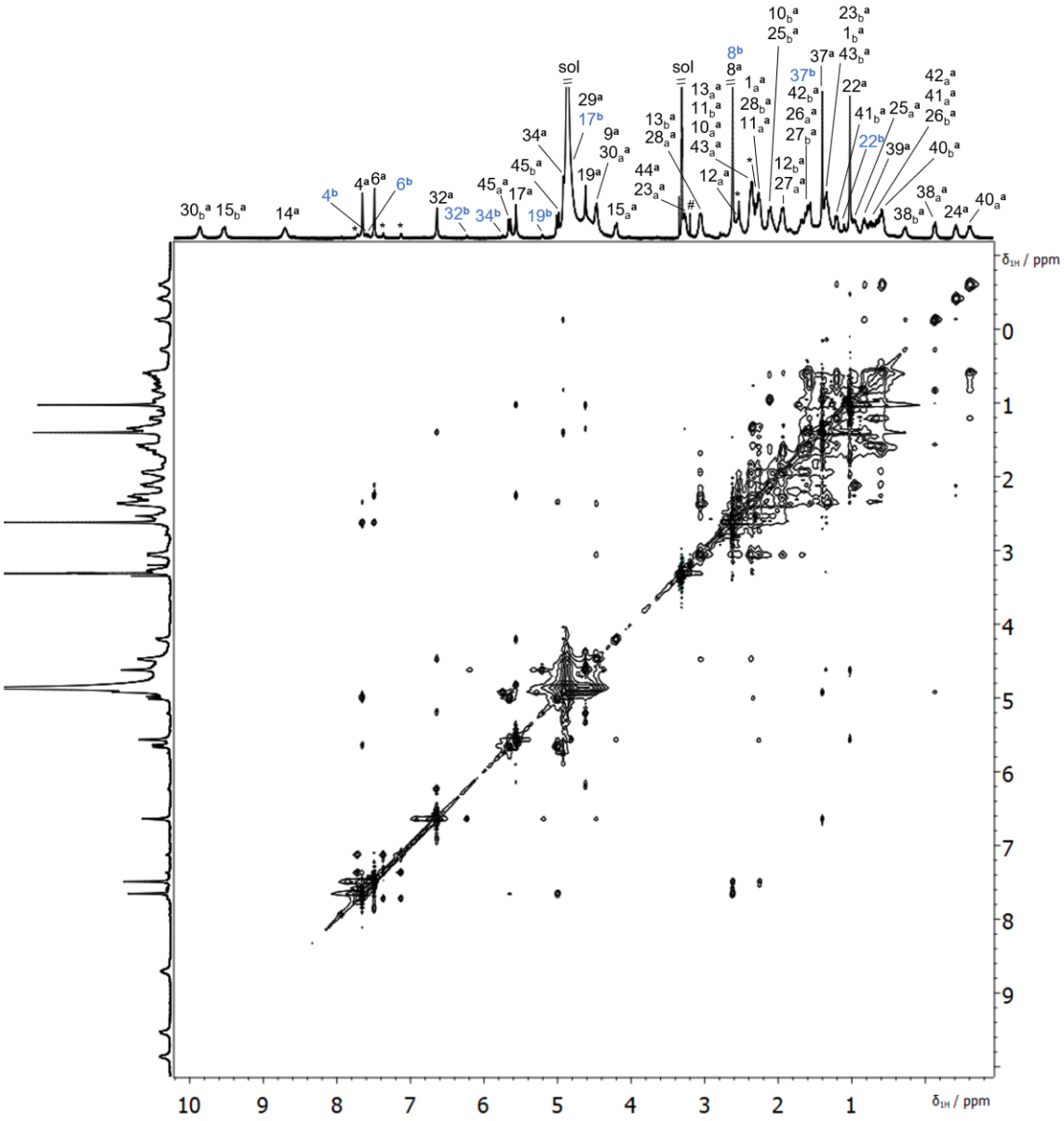

Figure S25 The NOESY spectrum (500 MHz, 300 K) obtained upon dissolving of **1a** in CD_3OD/D_2O 20:1 (v/v) mixture ($[\mathbf{1a}]_0$ = 16.5 mM). The signals of coordination species **1a**, **1b**, and **1c** were labeled with a superscript “a”, “b” or by an asterisk, respectively. Octothorpe denote signals of the impurities; signals sol of solvents.

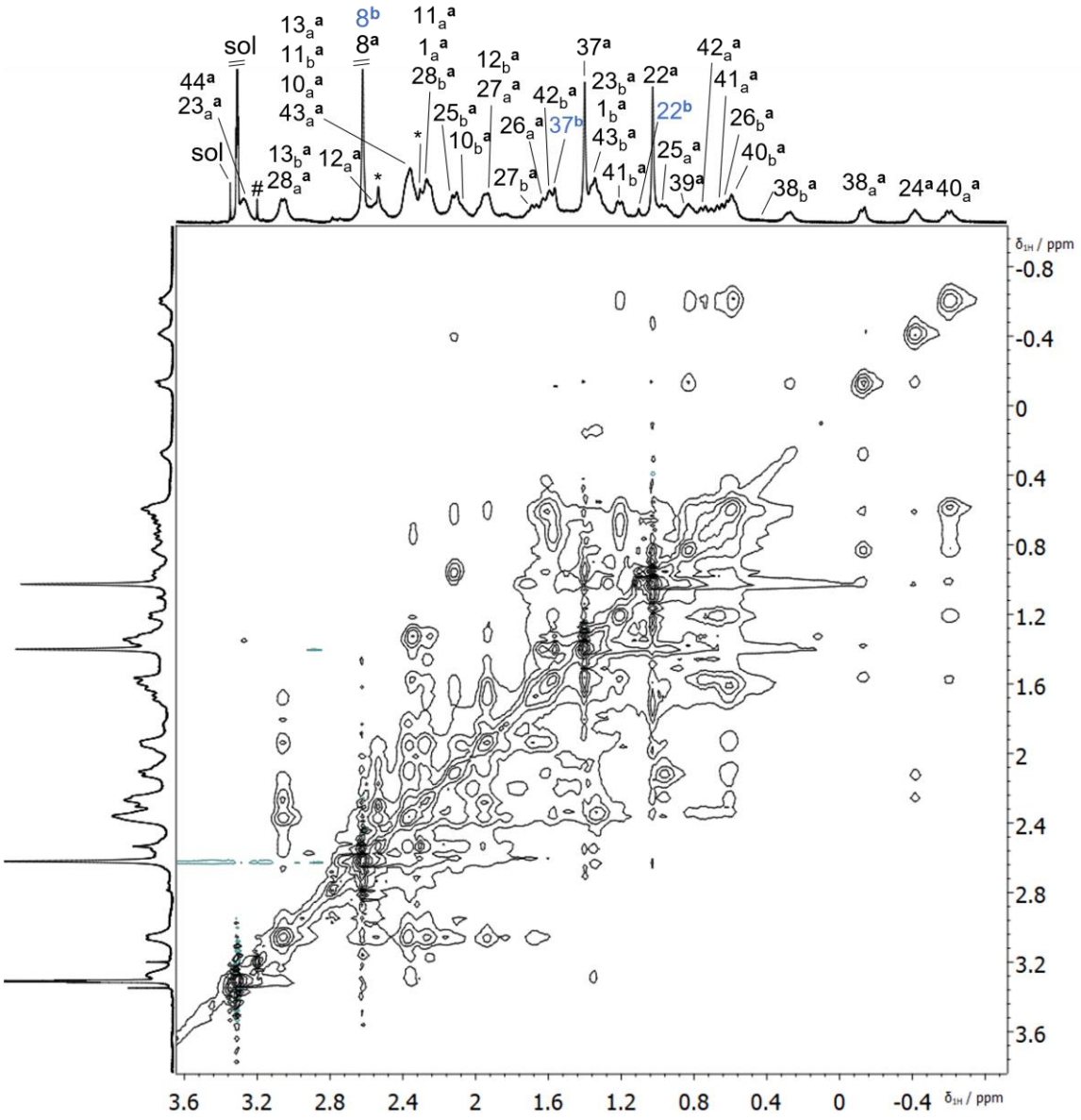

Figure S26 Aliphatic region of the NOESY spectrum (500 MHz, 300 K) of **1a** dissolved in CD_3OD/D_2O 20:1 (v/v) mixture ($[\mathbf{1a}]_0$ = 16.5 mM) shown with enhanced intensity. The signals of coordination species **1a**, **1b**, and **1c** were labeled with a superscript "a", "b" or by an asterisk, respectively. Octothorpe denote signals of the impurities; signals sol of solvents.

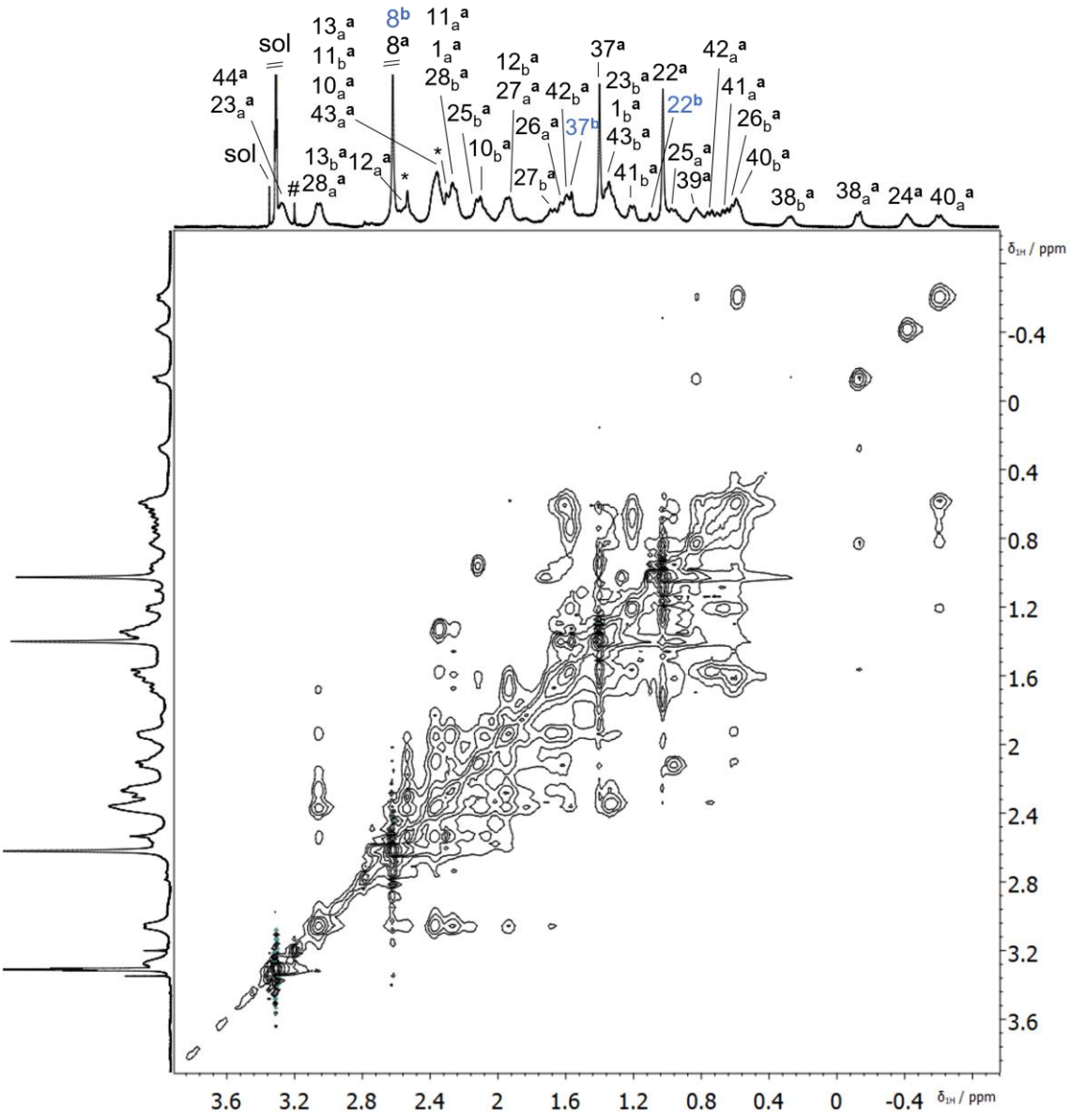

Figure S27 Aliphatic region of the NOESY spectrum (500 MHz, 300 K) of **1a** dissolved in CD_3OD/D_2O 20:1 (v/v) mixture ($[\mathbf{1a}]_0$ = 16.5 mM) shown with medium intensity. The signals of coordination species **1a**, **1b**, and **1c** were labeled with a superscript "a", "b" or by an asterisk, respectively. Octothorpe denote signals of the impurities; signals sol of solvents.

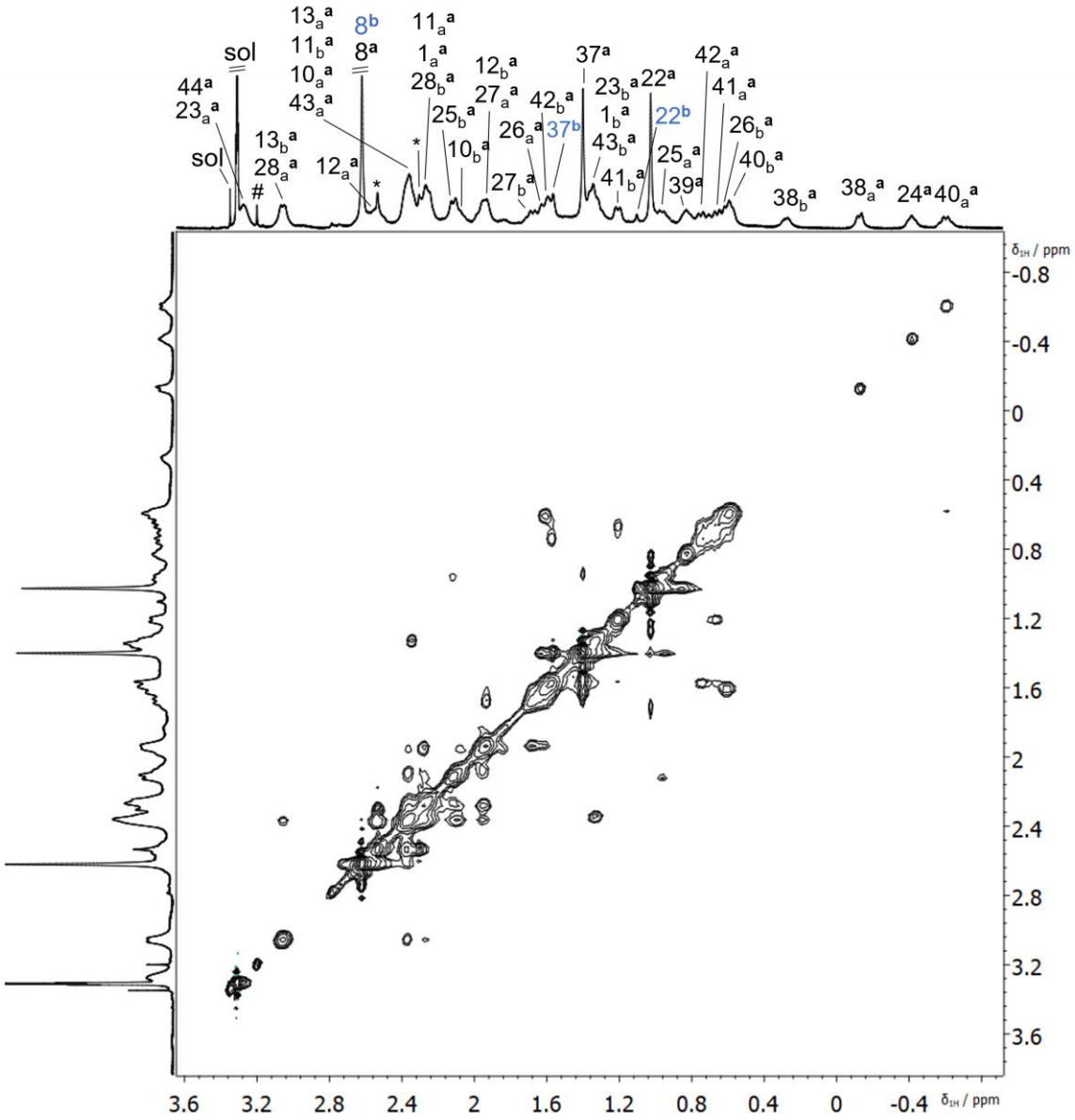

Figure S28 Part of the NOESY spectrum (500 MHz, 300 K) of **1a** dissolved in CD_3OD/D_2O 20:1 (v/v) mixture ($[\mathbf{1a}]_0$ = 16.5 mM) shown with reduced intensity. The signals of coordination species **1a**, **1b**, and **1c** were labeled with a superscript "a", "b" or by an asterisk, respectively. Octothorpe denote signals of the impurities; signals sol of solvents.

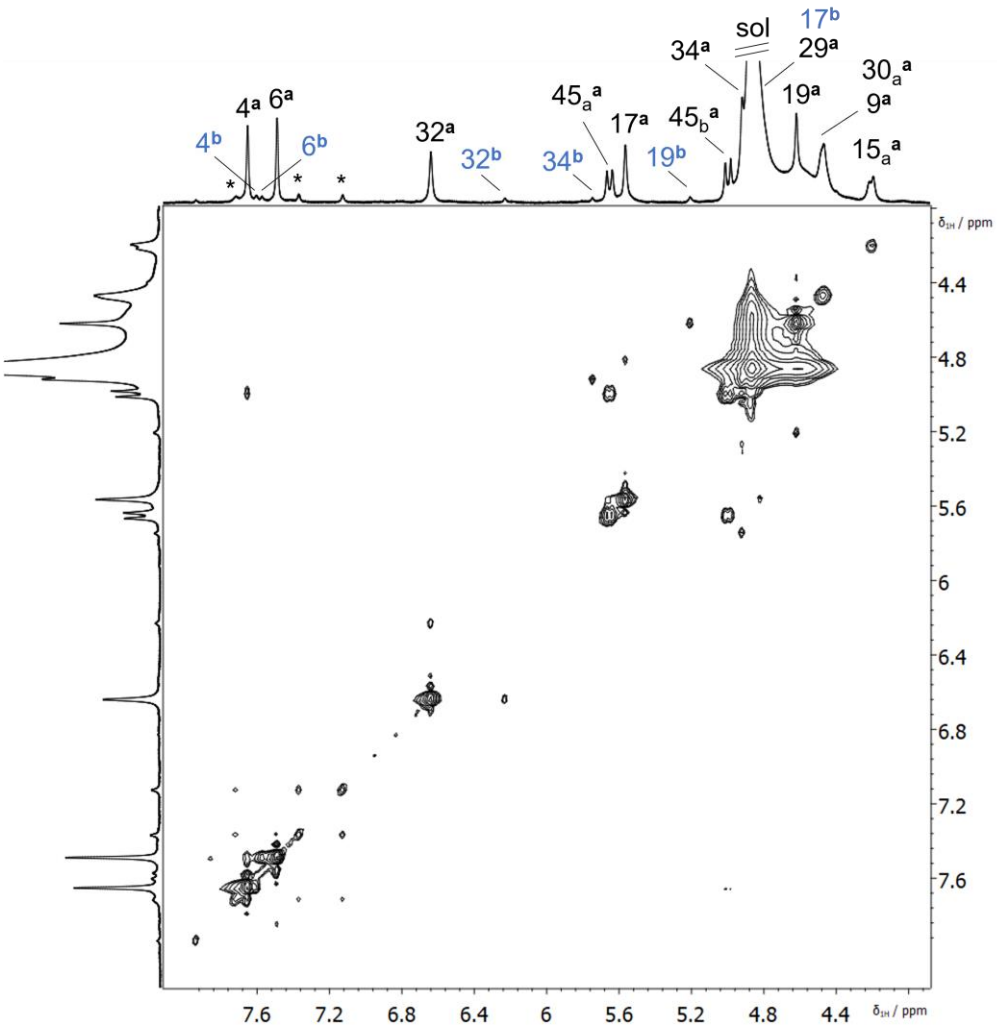

Figure S29 Aromatic part of the NOESY spectrum (500 MHz, 300 K) of **1a** dissolved in CD_3OD/D_2O 20:1 (v/v) mixture ($[\mathbf{1a}]_0$ = 16.5 mM) shown with reduced intensity. The signals of coordination species **1a**, **1b**, and **1c** were labeled with a superscript "a", "b" or by an asterisk, respectively. Signal of solvent was denoted as sol.

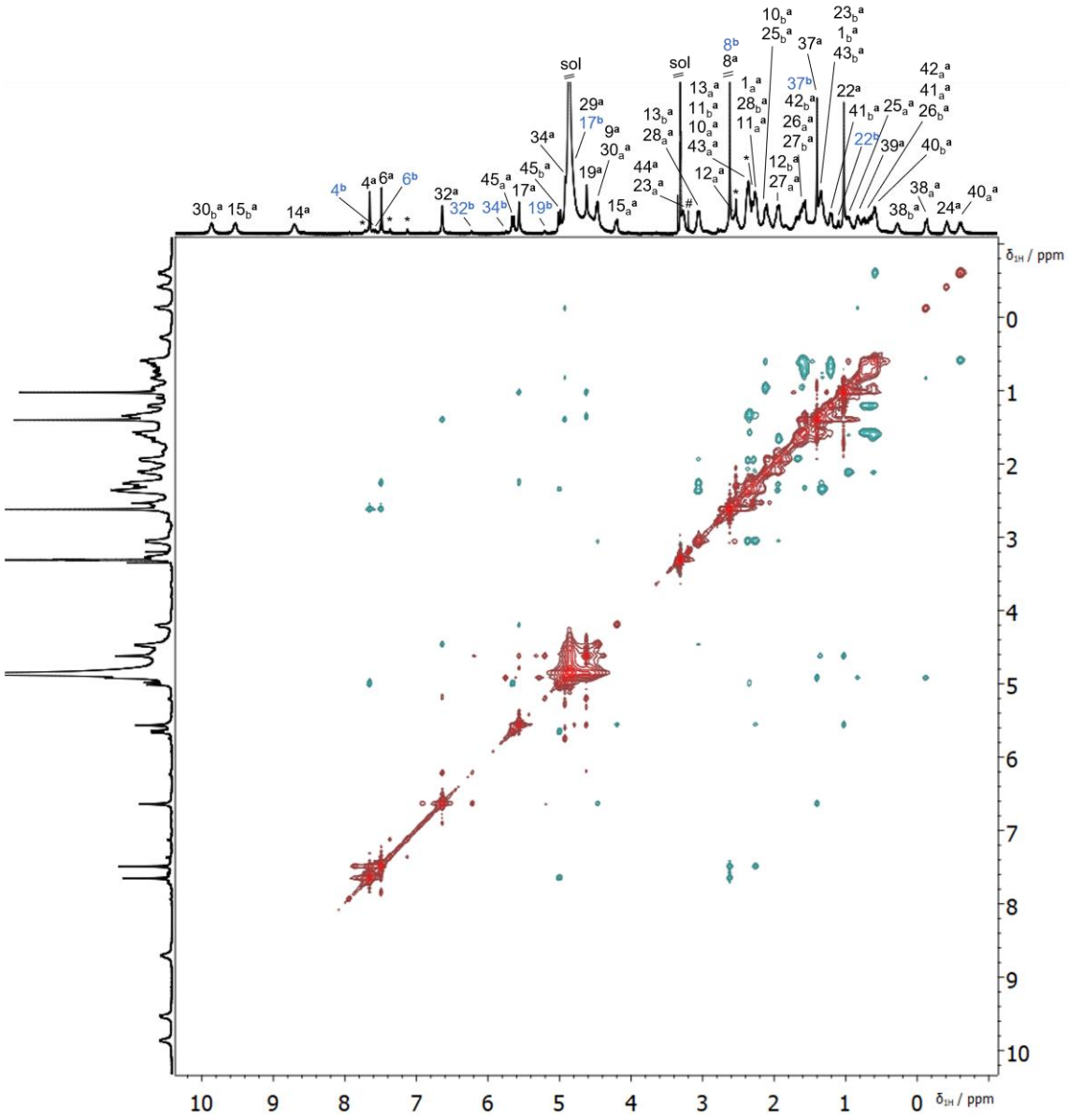

Figure S30 The ROESY spectrum (500 MHz, 300 K) obtained upon dissolving of **1a** in CD_3OD/D_2O 20:1 (v/v) mixture ($[\mathbf{1a}]_0$ = 16.5 mM). The signals of coordination species **1a**, **1b**, and **1c** were labeled with a superscript "a", "b" or by an asterisk, respectively. Octothorpe denote signals of the impurities; signals sol of solvents.

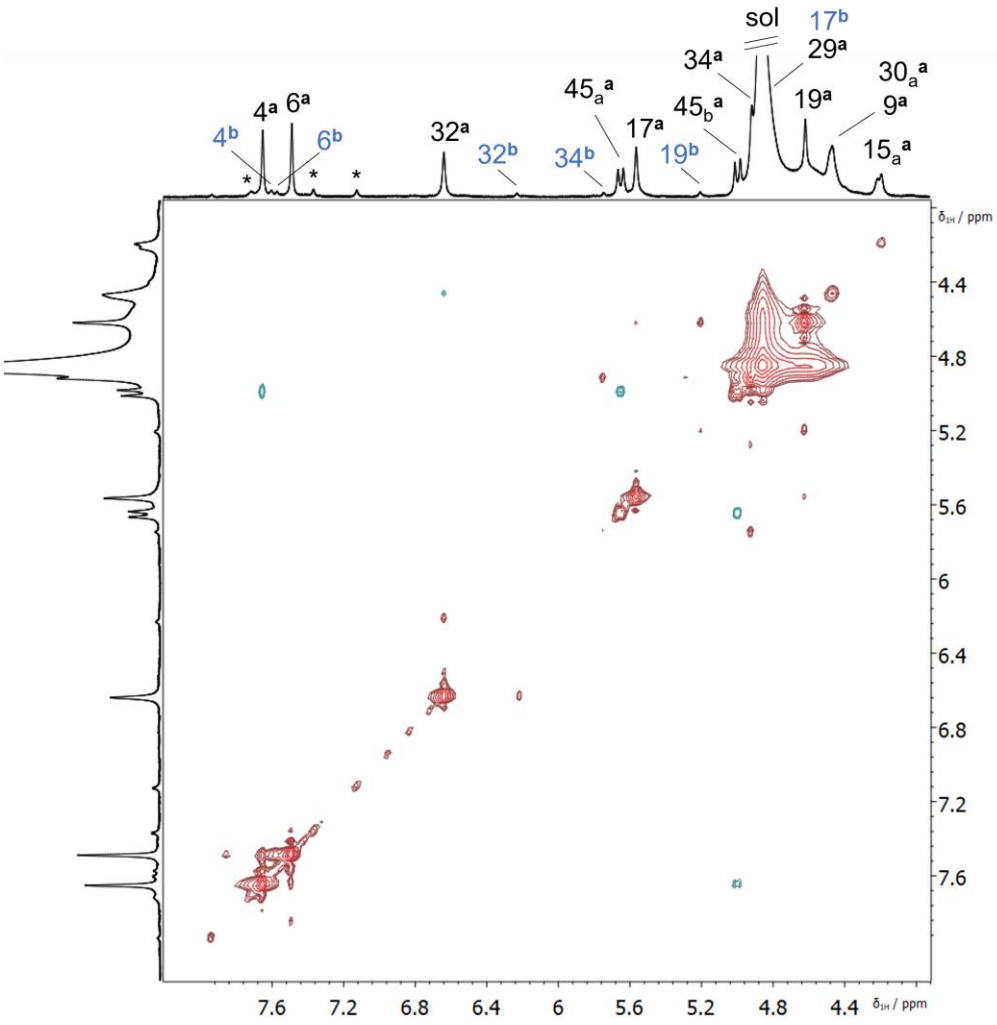

Figure S31 Aromatic region of the ROESY spectrum (500 MHz, 300 K) of **1a** dissolved in CD_3OD/D_2O 20:1 (v/v) mixture ($[\mathbf{1a}]_0$ = 16.5 mM) shown with reduced intensity. The signals of coordination species **1a**, **1b**, and **1c** were labeled with a superscript "a", "b" or by an asterisk, respectively. Signal of solvent was denoted as sol.

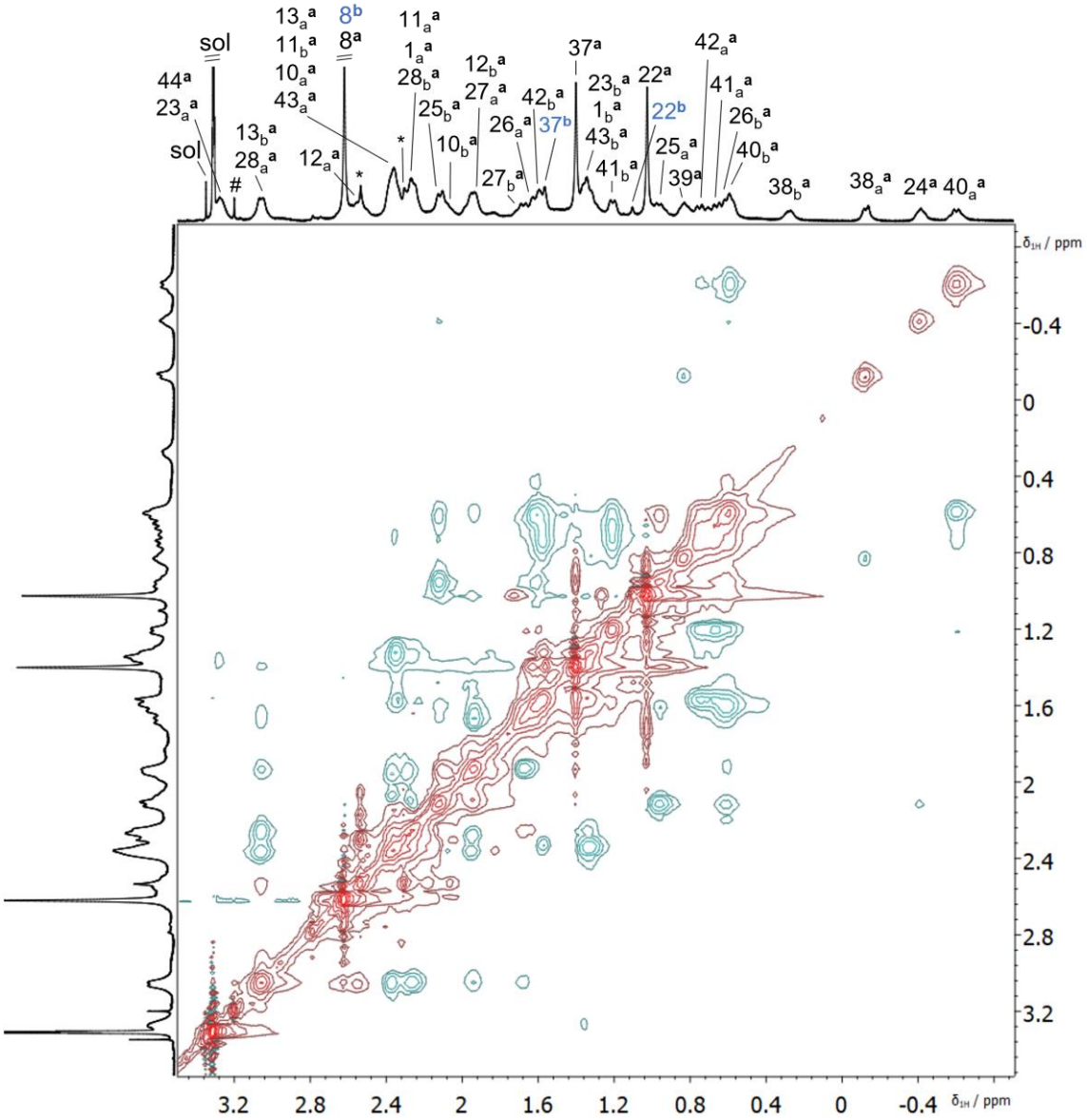

Figure S32 Aliphatic region of the ROESY spectrum (500 MHz, 300 K) of **1a** dissolved in CD_3OD/D_2O 20:1 (v/v) mixture ([**1a**]$_0$ = 16.5 mM) shown with enhanced intensity. The signals of coordination species **1a**, **1b**, and **1c** were labeled with a superscript "a", "b" or by an asterisk, respectively. Octothorpe denote signals of the impurities; signals sol of solvents.

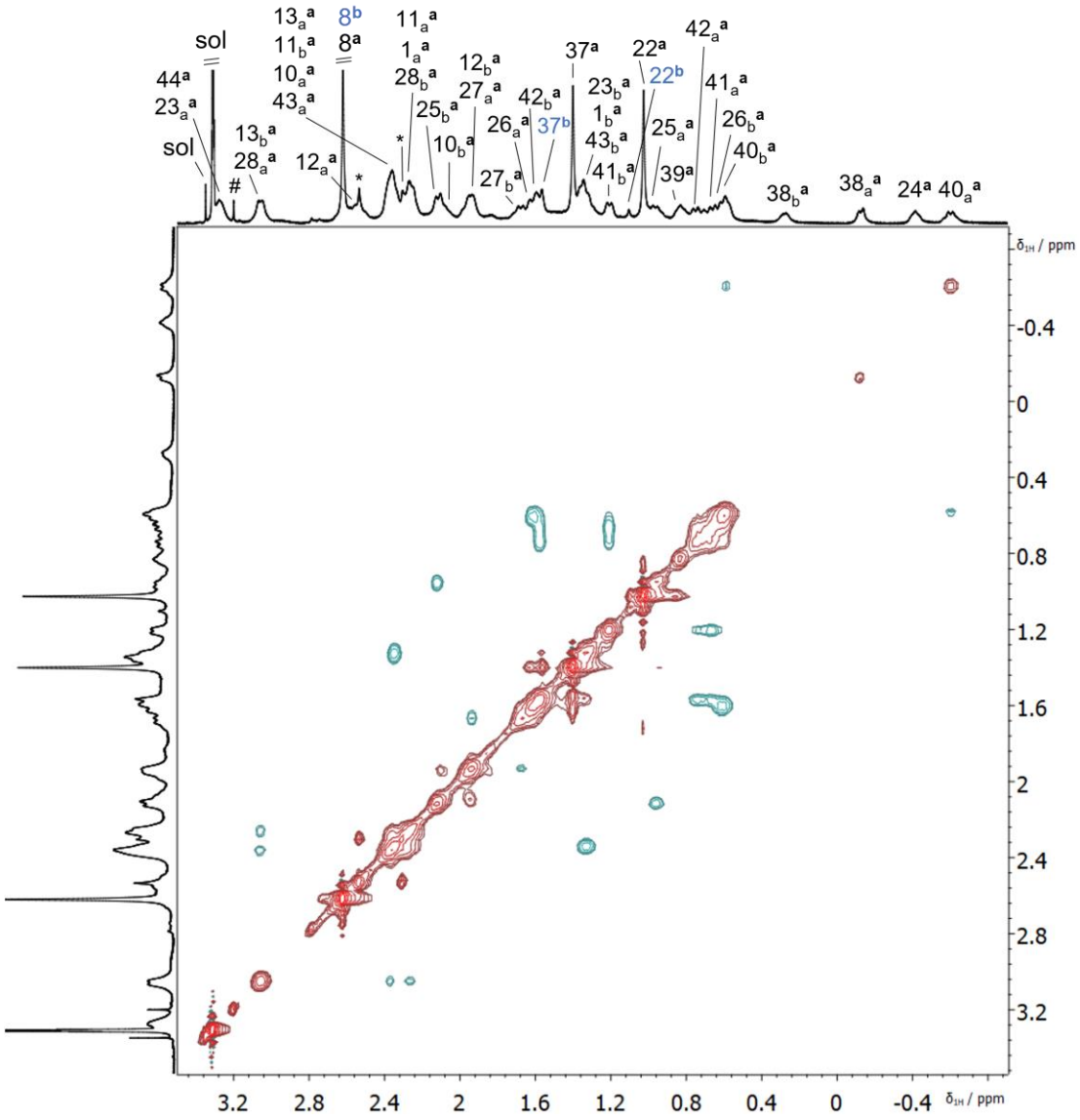

Figure S33 Aliphatic region of the ROESY spectrum (500 MHz, 300 K) of **1a** dissolved in CD_3OD/D_2O 20:1 (v/v) mixture ($[\mathbf{1a}]_0$ = 16.5 mM) shown with reduced intensity. The signals of coordination species **1a**, **1b**, and **1c** were labeled with a superscript "a", "b" or by an asterisk, respectively. Octothorpe denote signals of the impurities; signals sol of solvents.

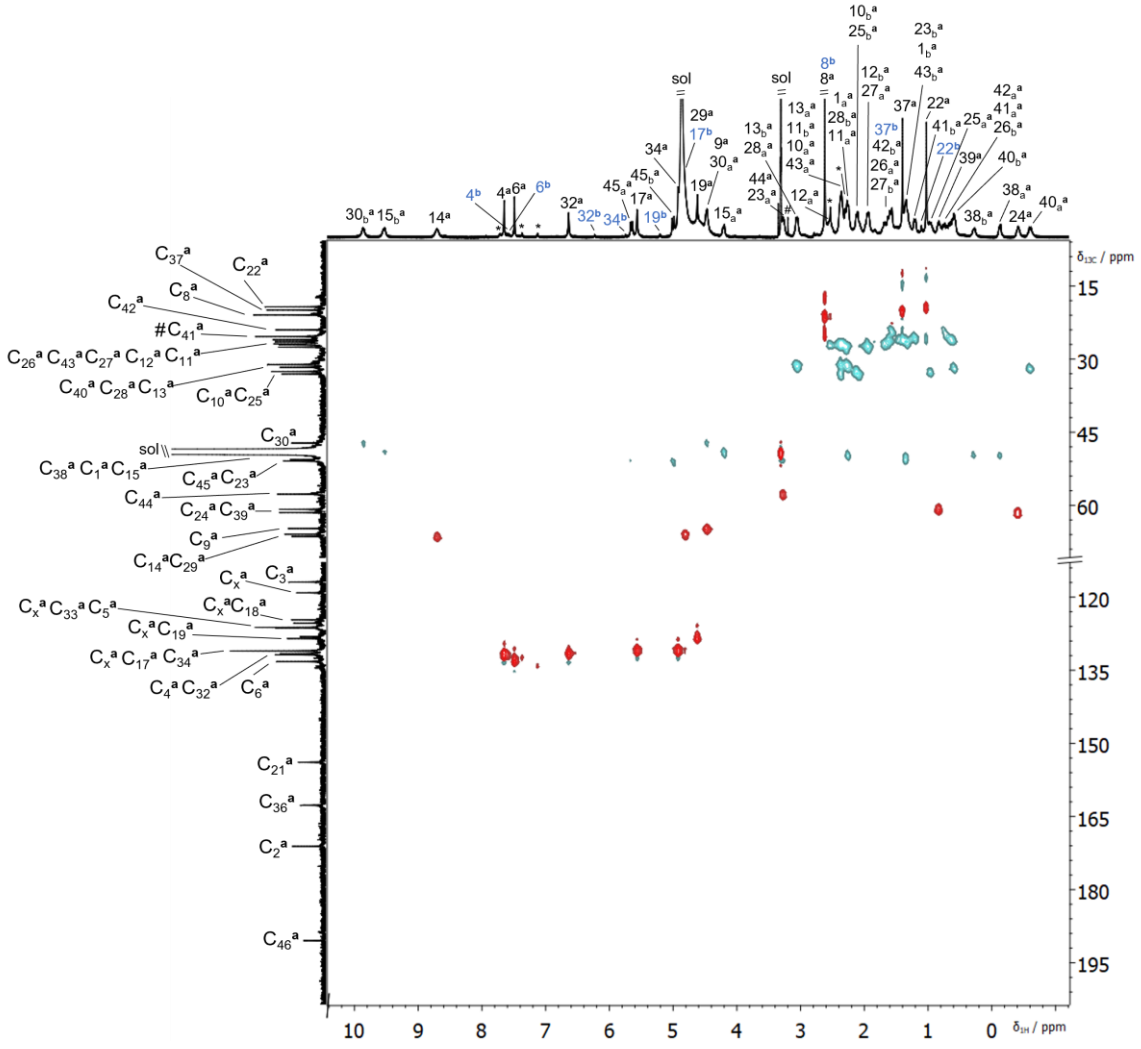

Figure S34 The HSQC spectrum obtained upon dissolving of **1a** in CD_3OD/D_2O 20:1 (v/v) mixture (300 K, $[\mathbf{1a}]_0$ = 16.5 mM). The signals of coordination species **1a**, **1b**, and **1c** were labeled with a superscript "a", "b" or by an asterisk, respectively. Octothorpe denote signals of the impurities; signals sol of solvents.

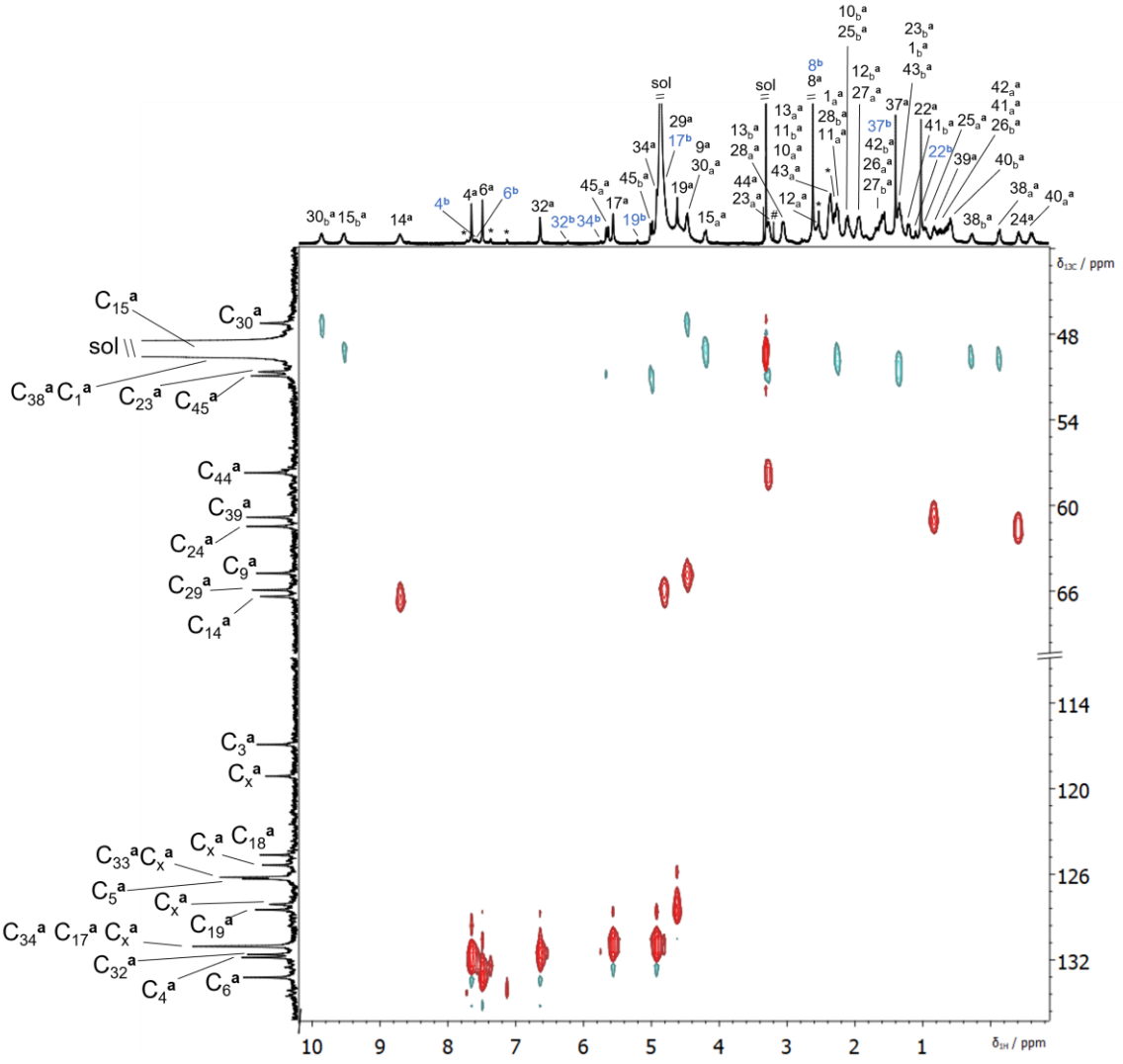

Figure S35 Part of the HSQC spectrum of **1a** dissolved in CD_3OD/D_2O 20:1 (v/v) mixture (300 K, $[\mathbf{1a}]_0$ = 16.5 mM). The signals of coordination species **1a**, **1b**, and **1c** were labeled with a superscript "a", "b" or by an asterisk, respectively. Octothorpe denote signals of the impurities; signals sol of solvents.

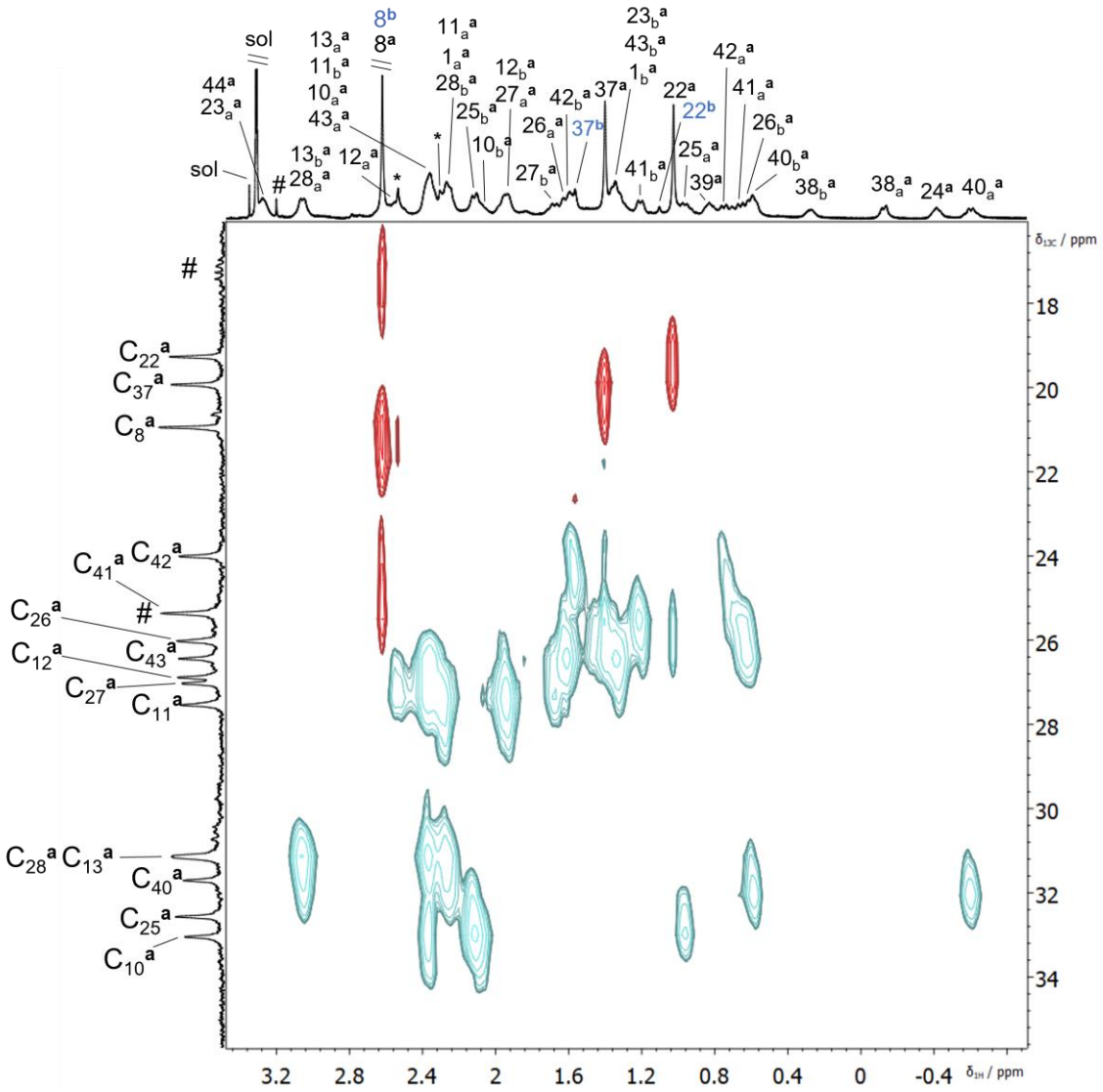

Figure S36 Aliphatic region of the HSQC spectrum of **1a** dissolved in CD_3OD/D_2O 20:1 (v/v) mixture (300 K, $[\mathbf{1a}]_0$ = 16.5 mM). The signals of coordination species **1a**, **1b**, and **1c** were labeled with a superscript "a", "b" or by an asterisk, respectively. Octothorpe denote signals of the impurities; signals sol of solvents.

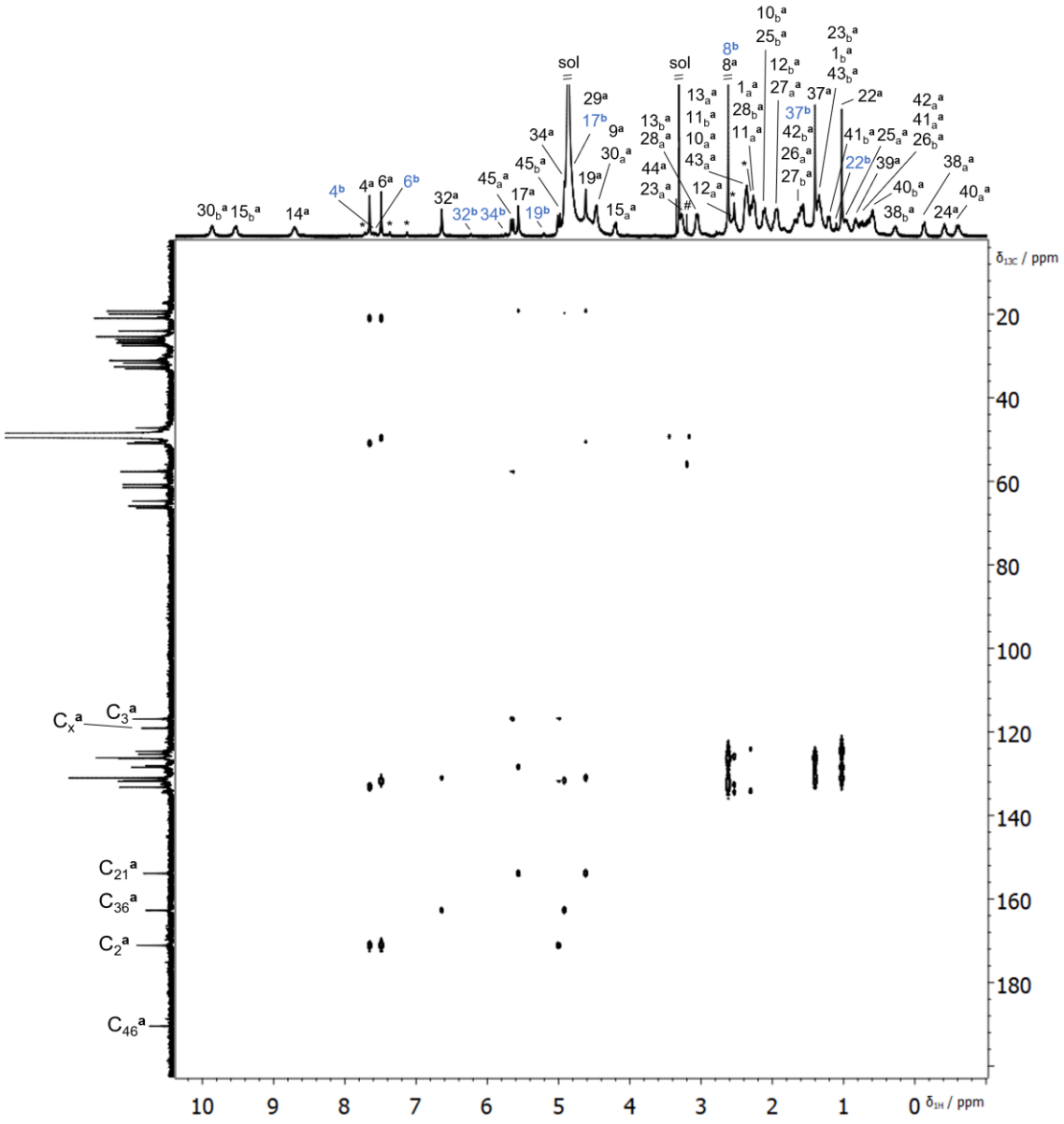

Figure S37 The HMBC of spectrum obtained upon dissolving of **1a** in CD_3OD/D_2O 20:1 (v/v) mixture (300 K, $[\mathbf{1a}]_0$ = 16.5 mM). The signals of coordination species **1a**, **1b**, and **1c** were labeled with a superscript "a", "b" or by an asterisk, respectively. Octothorpe denote signals of the impurities; signals sol of solvents.

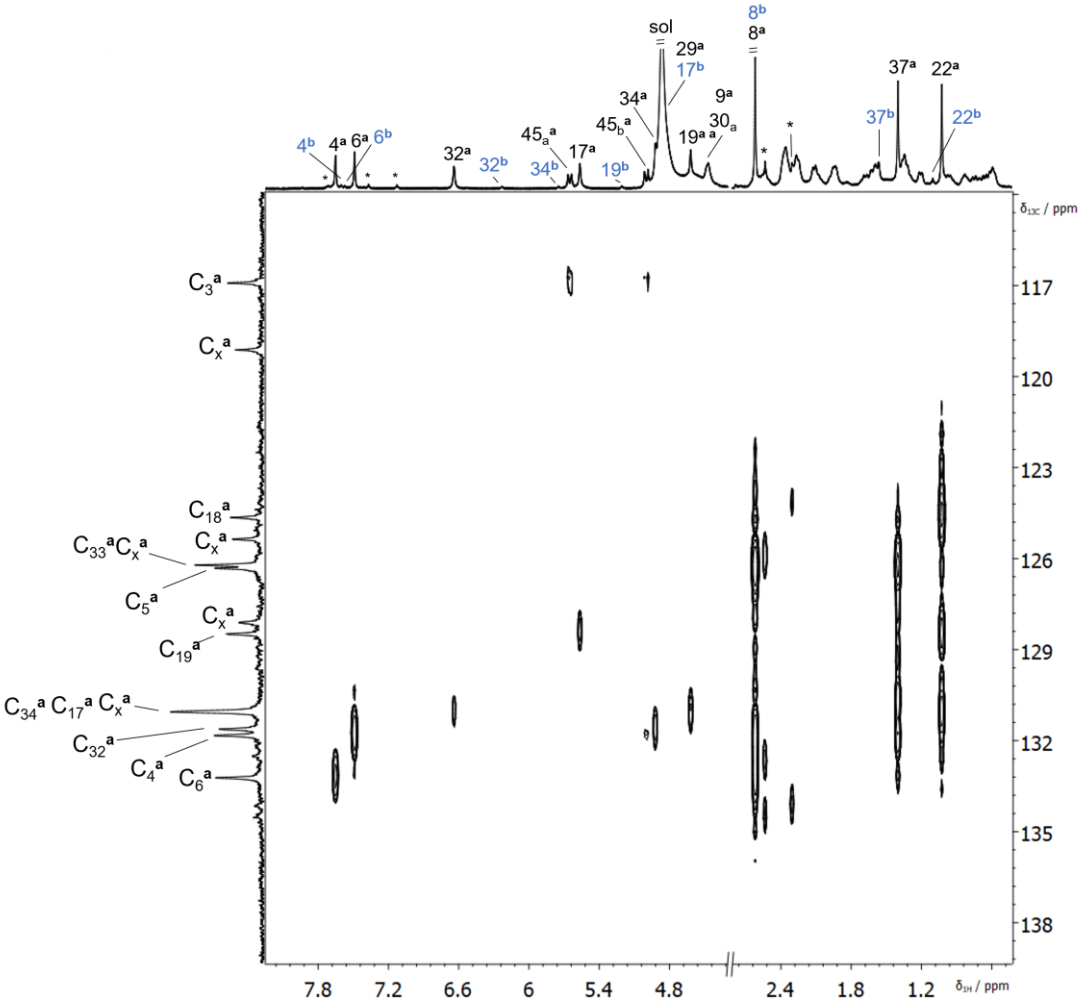

Figure S38 Part of the HMBC of spectrum of **1a** dissolved in CD_3OD/D_2O 20:1 (v/v) mixture (300 K, $[\mathbf{1a}]_0$ = 16.5 mM). The signals of coordination species **1a**, **1b**, and **1c** were labeled with a superscript “a”, “b” or by an asterisk, respectively. The signals of solvent was denoted with sol.

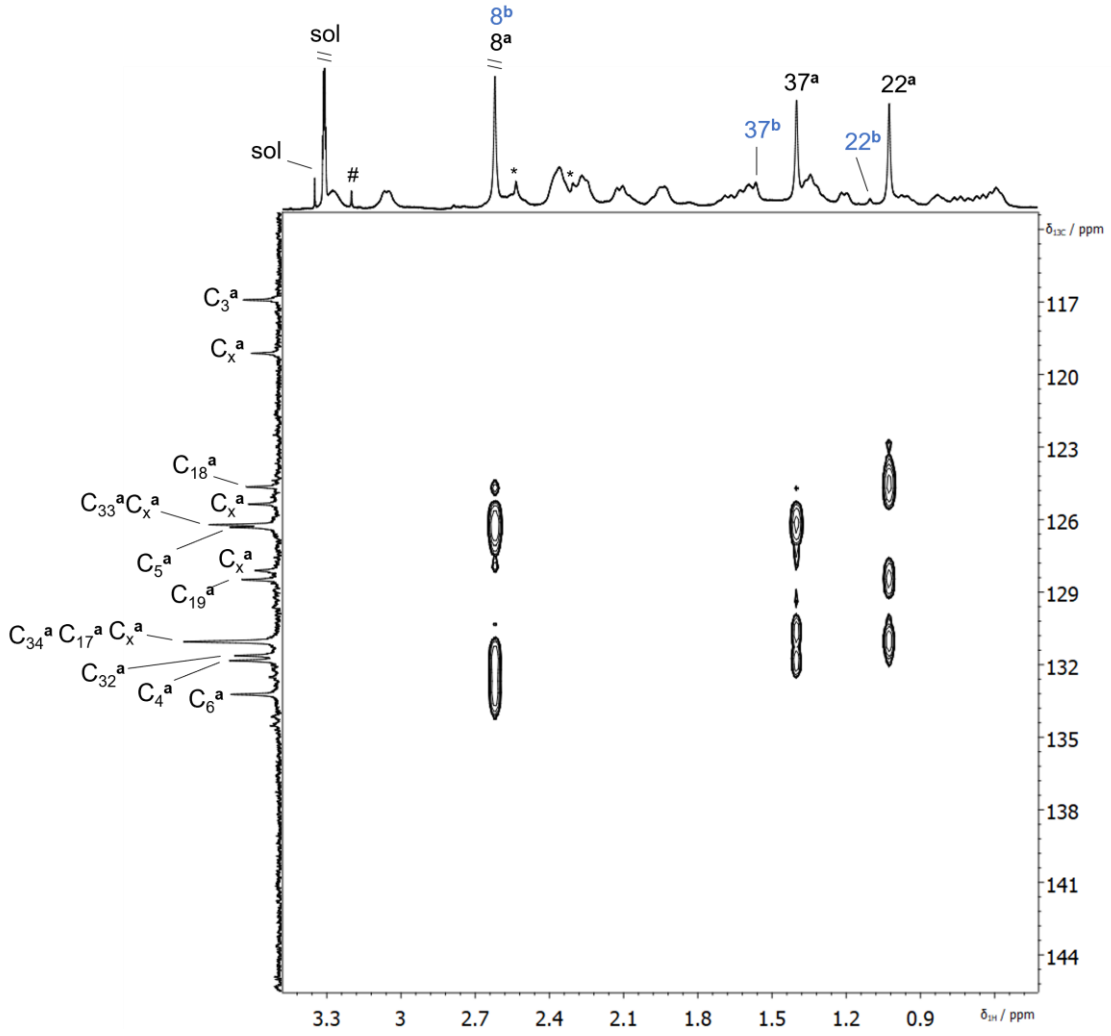

Figure S39 Part of the HMBC spectrum of **1a** dissolved in CD_3OD/D_2O 20:1 (v/v) mixture (300 K, $[\mathbf{1a}]_0$ = 16.5 mM) shown with reduced intensity. The signals of coordination species **1a**, **1b**, and **1c** were labeled with a superscript "a", "b" or by an asterisk, respectively. Octothorpe denote signals of the impurities; signals sol of solvent.

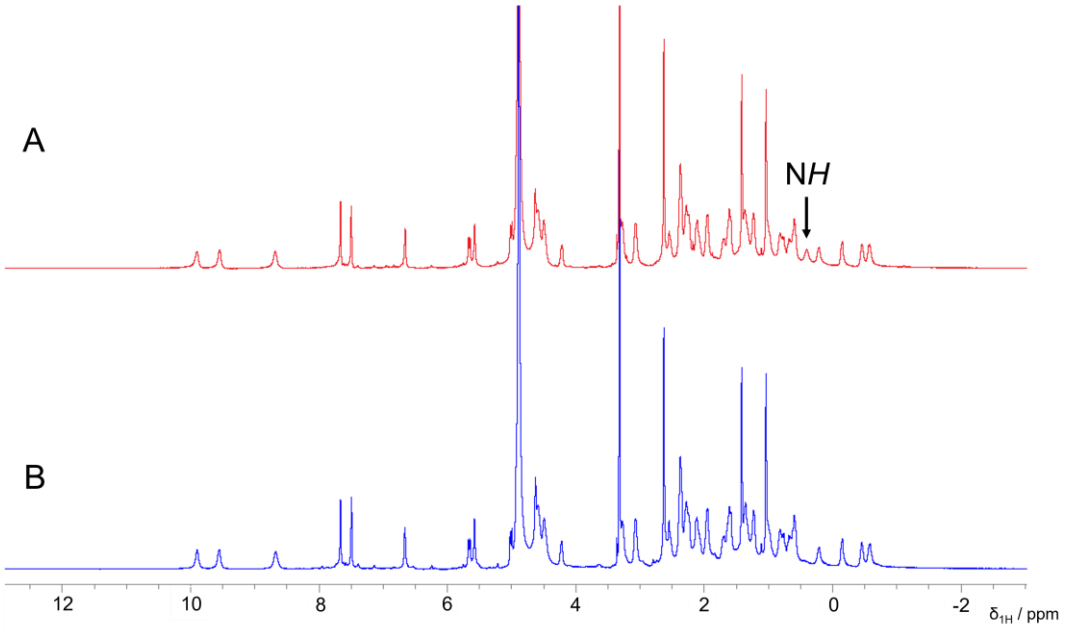

Figure S40 (**A**) The ^{1}H NMR spectrum (CD_3OD/D_2O 20:1, [**1a**]$_0$ = 9.2 mM, 600 MHz, 300 K) of $[Sm_4(HL^R)_2(CO_3)_2(NO_3)_2(H_2O)_4](NO_3)_2$ (**1a**) recorded immediately after dissolution of the sample. The NH signal was indicated by arrow. (**B**) The ^{1}H NMR spectrum (CD_3OD/D_2O 20:1, [**1a**]$_0$ = 9.2 mM, 600 MHz, 300 K) of deuterated form of **1a**, $[Sm_4(DL^R)_2(CO_3)_2(NO_3)_2(D_2O)_4](NO_3)_2$, measured immediately after dissolution of the sample. The deuterated form of the complex was synthesized by first dissolving the free macrocycle H_3L^R in CD_3OD/D_2O solvent mixture to ensure that all NH and OH positions become ND and OD positions and then repeating the reaction of complex formation.

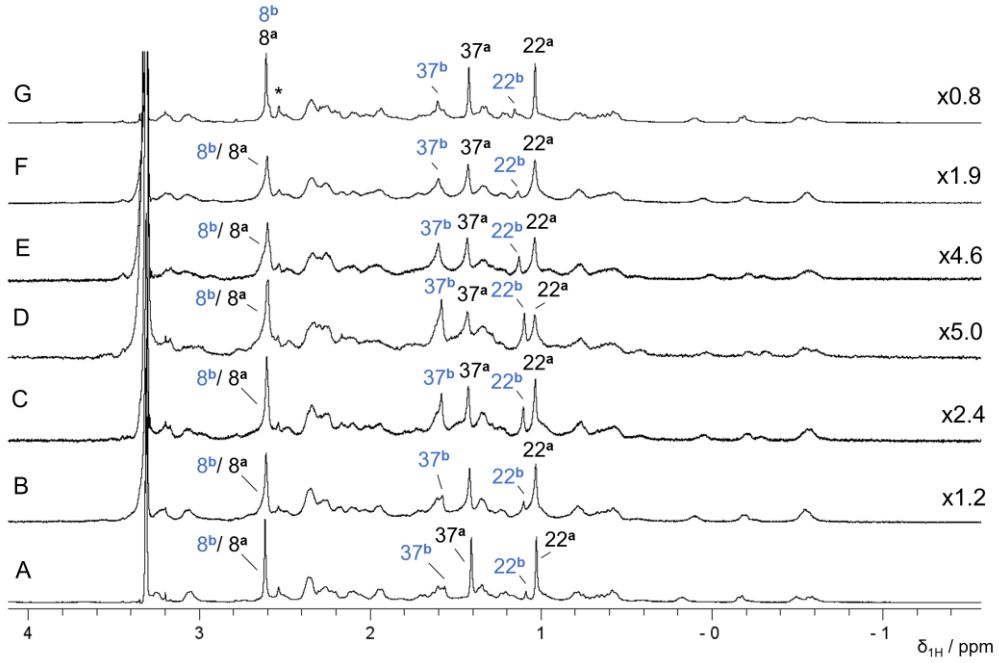

Figure S41 (A) Aliphatic region of the ^{1}H NMR spectrum (CD_3OD/D_2O 20:1 (v/v), [**1a**]$_0$ = 5.5 mM, 500 MHz, 300 K) of **1a**. The ^{1}H NMR spectra of the solution recorded after (B) 2-fold ([**1a**]$_0$ = 2.8 mM), (C) 4-fold ([**1a**]$_0$ = 1.4 mM), (D) 8-fold ([**1a**]$_0$ = 0.7 mM) dilution and total addition of (E) 1.4 mg ([**1a**]$_0$ = 2.0 mM), (F) 3.8 mg ([**1a**]$_0$ = 4.2 mM), and (G) 10.0 mg ([**1a**]$_0$ = 9.8 mM) of the sample.

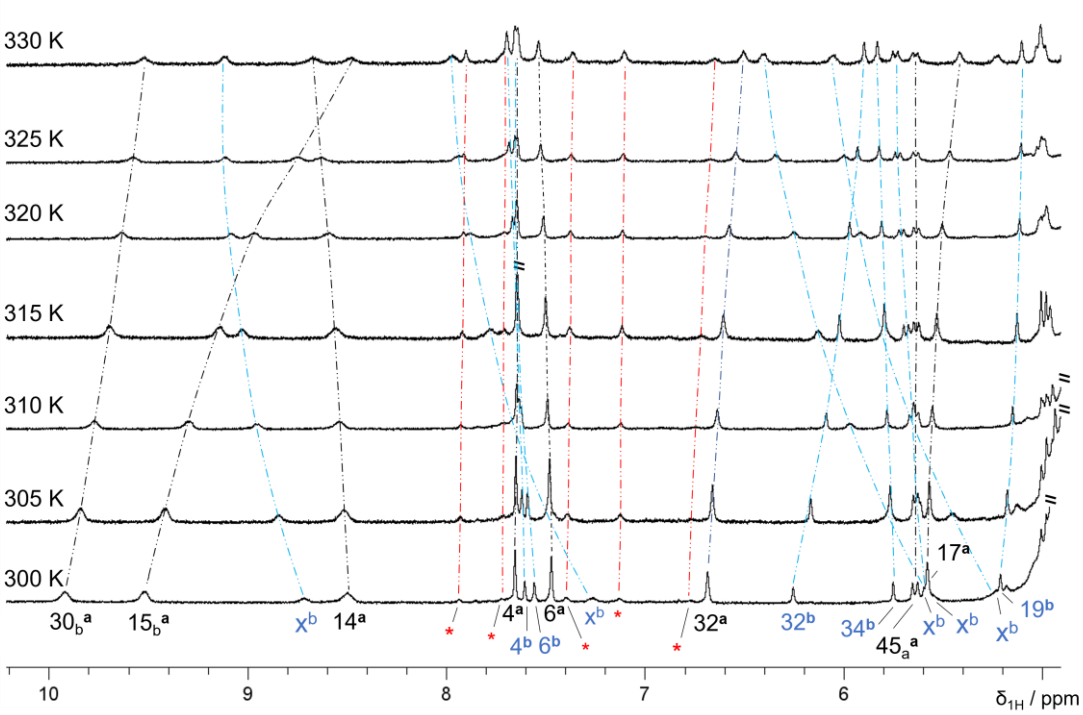

Figure S42 (From bottom) The ^{1}H NMR spectra of the **1a**/**1b**/**1c** mixture, obtained upon dissolving of **1a** in CD_3OD/D_2O 20:1 (v/v) (600 MHz, $[\mathbf{1a}]_0$ = 1.4 mM), recorded in 300-330 K temperature range. The signals of coordination species **1a** and **1b** were labeled with a superscript "a" and "b", respectively. Additional minor signals labelled by an asterisk correspond to mononuclear species **1c**, these signals increase with rising the temperature, suggesting the presence of further dissociation processes.

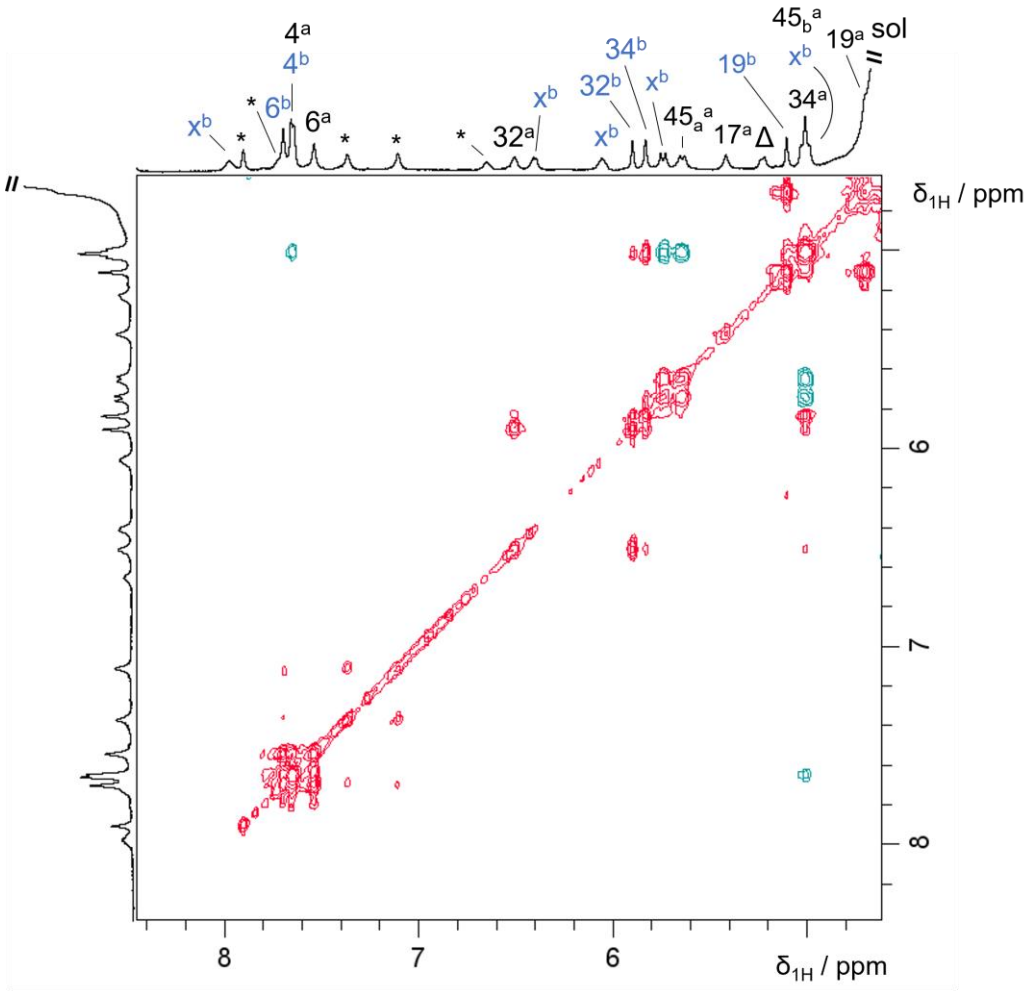

Figure S43 Phenyl region of the ROESY spectrum (600 MHz, 330 K) of **1a** dissolved in CD_3OD/D_2O 20:1 (v/v) mixture ($[\mathbf{1a}]_0$ = 1.4 mM) shown with reduced intensity. The signals of coordination species **1a**, **1b**, and **1c** were labeled with a superscript "a", "b" or by an asterisk, respectively. Delta denotes the unassigned signal corresponding to one of the detected coordination forms (**1a**, **1b** or **1c**). Signal of solvent was denoted as sol.

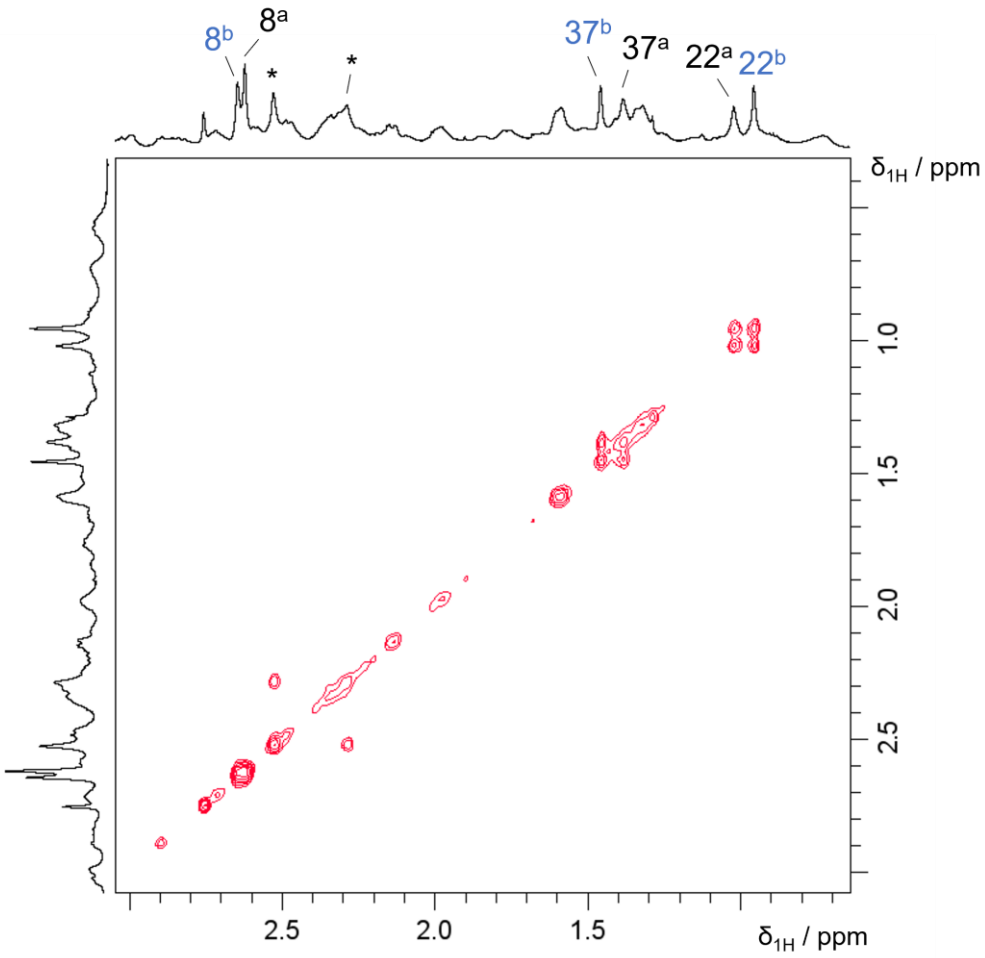

Figure S44 Aliphatic region of the ROESY spectrum (CD_3OD/D_2O 20:1 (v/v), $[\mathbf{1a}]_0$ = 1.4 mM, 600 MHz, 330 K) of **1a** shown with reduced intensity, which reveals the EXSY correlations between methyl protons of **1a** and **1b,** or **1c**. The methyl signals of the respective coordination forms were labeled with a superscript "a", "b" or by an asterisk.

8 References

1. K. Wydra, M. J. Kobyłka, T. Lis, K. Ślepokura, J. Lisowski, *Eur. J. Inorg. Chem.*, 2020, 2096-2104.
2. S. R. Korupoju, P. S. Zacharias, *Chem Commun.*, 1998, 1267-1268.
3. J. Gao, R. A. Zingaro, J. H. Reibenspies, A. E. Martell, *Org. Lett.*, 2004, **6**, 14, 2453-2455.
4. CrysAlisPro, Rigaku OD, 2020.
5. G. M. Sheldrick, *Acta Crystallogr., Sect. A* 2008, **64**, 112–122.
6. G. M. Sheldrick, *Acta Crystallogr., Sect. C*, 2015, **71**, 3-8.
7. M. Llunell, D. Casanova, J. Cirera, P. Alemany, S. Alvarez, *SHAPE: Program for the Stereochemical Analysis of Molecular Fragments by Means of Continuous Shape Measures and Associated Tools*, version 2.1; Universitat de Barcelona: Barcelona, 2013.
8. M. Paluch, J. Lisowski, T. Lis, *Dalton Trans.*, 2006, 381-388.